University of Tennessee, Knoxville
Trace: Tennessee Research and Creative Exchange

Masters Theses | Graduate School

8-2007

Mechanisms of Organic Matter Preservation in Continental Margin Sediments from the Gulf of Maine

Laura A. Taylor
University of Tennessee, Knoxville

Recommended Citation

Taylor, Laura A., "Mechanisms of Organic Matter Preservation in Continental Margin Sediments from the Gulf of Maine. " Master's Thesis, University of Tennessee, 2007.
https://trace.tennessee.edu/utk_gradthes/4442

This Thesis is brought to you for free and open access by the Graduate School at Trace: Tennessee Research and Creative Exchange. It has been accepted for inclusion in Masters Theses by an authorized administrator of Trace: Tennessee Research and Creative Exchange. For more information, please contact trace@utk.edu.

To the Graduate Council:

I am submitting herewith a thesis written by Laura A. Taylor entitled "Mechanisms of Organic Matter Preservation in Continental Margin Sediments from the Gulf of Maine." I have examined the final electronic copy of this thesis for form and content and recommend that it be accepted in partial fulfillment of the requirements for the degree of Master of Science, with a major in .

Edmund Perfect, Major Professor

We have read this thesis and recommend its acceptance:

Linda Kah, John McCarthy

Accepted for the Council:
Dixie L. Thompson

Vice Provost and Dean of the Graduate School

(Original signatures are on file with official student records.)

To the Graduate Council:

I am submitting herewith a thesis written by Laura A. Taylor entitled "Mechanisms of Organic Matter Preservation in Continental Margin Sediments from the Gulf of Maine." I have examined the final paper copy of this thesis for form and content and recommend that it be accepted in partial fulfillment of the requirements for the degree of Master of Science, with a major in Earth and Planetary Science.

Edmund Perfect, Major Professor

We have read this thesis
and recommend its acceptance:

Linda Kah

John McCarthy

Acceptance for the Council:

Vice Provost and Dean of the Graduate School

Thesis
2007
.T43

Mechanisms of Organic Matter Preservation in Continental Margin Sediments from the Gulf of Maine

A Thesis Presented for the
Master of Science Degree
The University of Tennessee, Knoxville

Laura Ann Taylor
August 2007

Copyright © 2007 by Laura Ann Taylor
All rights reserved

DEDICATION

This thesis is dedicated to the many people who have supported me through all of life's obstacles and successes. My teachers such as Carolyn Eastman and Marty Paco, who pushed me beyond what I thought I could accomplish and taught me that learning can be fun. My mentors and friends Jim and Suzi Dressler, who have always given their love and guidance, without which I would not be the person I am today. To my parents Chris and Joyce Lieberman, for teaching me to be understanding, self aware, and to never stop learning. My brother Eric Lieberman for being my best friend through everything and giving me the love and support I did not always deserve.

I am especially grateful to my husband Zack for his boundless patience and encouragement during my time at the University of Tennessee.

ACKNOWLEDGEMENTS

I am grateful to a large number of people for their assistance and support throughout the entire thesis process. My advisor Edmund Perfect gave me the opportunity to work on this project and kept me on track. John McCarthy supervised the research conducted at the University of Tennessee. Linda Kah served on my committee and was instrumental in helping put my research in a broader geological context.

I would especially like to recognize professor Lawrence Mayer at the University of Maine for allowing me the opportunity to visit my study site and collect my own core samples. His patience and knowledge broadened my understanding of carbon sequestration in marine environments and improved my research. Linda Schick, from the University of Maine, was very helpful in teaching me the lab techniques and answering questions.

Professors Ken Orvis and Sally Horn allowed the use of their particle size analysis lab, without which the clay and silt separation process would have taken five times as long. Professor Dean Kopsell graciously allowed the use of his lyophilizer. Nancy Neilsen for teaching me about flow cytometry and volunteering her services. This thesis could not have been completed without her last minute help.

My colleague Tairone Leao was very helpful in suggesting solutions when problem aroses, and for that I thank him.

The Petroleum Research Fund provided funding for the project. I am also grateful to the Mayo Educational Foundation for awarding me a grant, which allowed me to travel to Walpole, Maine to recover and analyze the sediment cores.

ABSTRACT

Burial of organic carbon on marine shelves is an important process in the long-term sequestration of carbon from the marine carbon cycle. As organic matter in marine environments is consumed and resuspended by microorganisms, only a small portion is preserved. This organic material is preferentially associated with the fine-grained fraction of continental margin sediments. The strong correlation between organic matter content and fine-grained particles has led to speculation that organic matter may be adsorbed onto mineral surface and physically protected by incorporation into aggregates.

Two methods were used to determine the role of aggregates in the physical preservation of organic carbon in marine sediments from the Gulf of Maine. First, carbon storage potential was measured through a range of particle and aggregate sizes. Silt-size (2-53 μm) and clay-size (< 2 μm) fractions were isolated using settling columns, and separated by density into particles (ρ>2.3 g cm^{-1}) and aggregates (ρ<2.3 g cm^{-1}) using heavy liquid floatation. Systematic differences between preserved carbon content in silt and clay particle and aggregate fractions were determined by measuring organic carbon and specific surface area via a carbon analyzer and the nitrogen gas adsorption method. Second, differences in physical stability between silt and clay aggregates were measured. Relative size distributions of silt and clay aggregates were measured, via flow cytometry and x-ray disc centrifugation, before and after exposure to stepwise increasing levels of sonic energy.

The highest levels of organic carbon were associated with clay-sized aggregates, but aggregates in the silt-size fraction around 3 cm below the sediment water interface

appear to be the most physically stable. This suggests that although organic carbon is preferentially associated with aggregates, it may not be the sole mechanism controlling aggregate physical stability. Increased aggregate stability could be the result of physical process such as compaction, dewatering, lithification, and/or the quality of organic carbon beginning to occur around 3 cm of depth.

TABLE OF CONTENTS

ACKNOWLEDGEMENTS ..... **IV**

ABSTRACT ..... **V**

CHAPTER 1: INTRODUCTION **1**

CHAPTER 2: LITERATURE REVIEW **3**

ORGANIC CARBON IN MARINE ENVIRONMENTS 3
ORGANIC CARBON STORAGE AND STABILITY: ROLE OF AGGREGATES 4
OBJECTIVE OF THIS STUDY 8

CHAPTER 3: SAMPLE COLLECTION AND METHODS **10**

SAMPLE COLLECTION 10
OVERVIEW OF METHODS 10
PARTICLE DENSITY 13
PARTICLE SIZE DISTRIBUTION 14
DENSITY FRACTIONATION 15
MINERALOGICAL COMPOSITION 16
CARBON, NITROGEN, AND SPECIFIC SURFACE AREA MEASUREMENTS 16
AGGREGATE SIZE DISTRIBUTION AND STABILITY 17

CHAPTER 4: RESULTS **20**

PARTICLE DENSITY 20
PARTICLE SIZE DISTRIBUTION 20
MINERALOGICAL COMPOSITION 22
ORGANIC CARBON AND NITROGEN 22
SURFACE AREA MEASUREMENTS 26
SIZE DISTRIBUTION PRIOR TO SONICATION 28
Silt-Size Aggregate Fraction *30*
Clay-Size Aggregate Fraction *30*
SIZE DISTRIBUTION AFTER SONICATION 33
Aggregate Disruption with Increasing Sonic Energy *33*
Aggregate Disruption with 2000 J/mL of Sonic Energy *35*
Stability Ratios *37*

CHAPTER 5: INTERPRETATION AND DISCUSSION **39**

MINERALOGY 39
ORGANIC CARBON AND STABILITY 40
DISRUPTED AGGREGATES 41
LIMITATIONS OF ANALYTICAL TECHNIQUES 43

CHAPTER 6: CONCLUSIONS AND FUTURE RESEARCH **45**

REFERENCES **47**

APPENDICES **51**

APPENDIX A: PYCNOMETER DATA 52
APPENDIX B: XRF ELEMENTAL COMPOSITION OF THE BULK SEDIMENT 53
APPENDIX C: XRD MINERALOGICAL COMPOSITION 55
APPENDIX D: FLOW CYTOMETER DATA 59
APPENDIX E: XDC SIZE DATA 65

VITA 72

LIST OF FIGURES

Figure 2.1: SEM of Louisiana Bayou sediment showing drape of organic matter (O) across multiple mineral grains (d). 5

Figure 2.2: Diagram of multi-component aggregates. The numbers indicate individual aggregates sticking together to form a larger aggregate. 6

Figure 2.3. Micrographs obtained with an environmental SEM from Louisiana Bayou showing the high porosity and openness of structure a) 20 μm scale b) 5 μm scale. 7

Figure 3.1: Map of Gulf to Maine including watershed. The asterisk indicates the location were the sample was collected. 11

Figure 3.2: Flow chart outlining the steps performed in this study. 12

Figure 4.1: Cumulative percent of the particle size distribution for all seven sediment samples. 21

Figure 4.2: Organic carbon and surface area measurements for silt-size particles, silt-size aggregates, clay-size particles, and clay-size aggregates. 29

Figure 4.3: Cumulative percent graph for the silt-size aggregate fraction measured with the flow cytometer. 31

Figure 4.4: Cumulative percent graph for the silt-size aggregate fraction measured with the XDC. 31

Figure 4.5: Cumulative percent graph for the clay-size aggregate fraction measured with the flow cytometer. 32

Figure 4.6: Cumulative percent graph for the clay-size aggregate fraction measured with the XDC. 32

Figure 4.7: Cumulative percent graph created from the flow cytometer data for the silt-size aggregate fraction sonicated with increasing levels of sonic energy. Curves plotted and compared to the non-sonicated silt-and clay-size aggregate fraction. 34

Figure 4.8: Cumulative percent graph created from the flow cytometer data for the silt-size aggregate fraction sonicated with 2000 J/mL of sonic energy. 36

Figure 4.9: Stability ratios versus organic carbon content for the disrupted silt-size aggregates fraction. 38

Figure 4.10: Stability ratios for the silt-size aggregates sonicated at 2000 J/mL of energy plotted against organic carbon content. 38

LIST OF TABLES

Table 3.1: Chemical composition of seawater mixed using Instant Ocean compared to natural seawater. 450 grams of powdered Instant Ocean was added to 3800 mL of deionized water. 14

Table 4.1: Particle density calculated using the Pycnometer method. 20

Table 4.2: Organic carbon, nitrogen, and C:N ratios for silt-size particles, silt-size aggregates, clay-size particles, and clay-size aggregates. 23

Table 4.3: Specific surface area measurements for silt-size particles, silt-size aggregates, clay-size particles, and clay-size aggregates. 25

Table 4.4: Paired T-test results between fractions and (1) surface area measurements before and after organic matter removal, (2) surface area measurements with organic carbon removed, and (3) OC:SFA. SP=silt-size particle, SA=silt-size aggregates, CP=clay-size particle, and CA=clay-size aggregate. b is SFA before OC removal and a is SFA after OC removal. 28

Table 4.5: XDC equivalent diameter (μm) of 50 percent of the silt-size aggregates, clay-size aggregates, and silt-size aggregate sonicated with 2000 J of energy. Stability ratios are listed for the sonicated silt-size aggregates. 37

CHAPTER 1: INTRODUCTION

Understanding organic carbon sequestration in marine sediments is critical to developing accurate models of global carbon cycling. In turn, these models can improve our understanding of climate response to anthropogenic carbon input, decadal to millennial-scale climate change, and even the effect of carbon cycling at geologic time scales (DE HAAS et al., 2002; KEIL et al., 1994). Presently this work is hindered because the factors controlling organic matter preservation in marine environments are not well understood (KEIL et al., 1994).

Many of the processes that govern carbon storage have been identified and characterized in the terrestrial realm where access to sampling sites is relatively easy (HEDGES and OADES, 1997; KRULL et al., 2003). In soils, organic matter is physically protected by its association with the surrounding soil matrix (BALDOCK and NELSON, 1999; BALDOCK and SKJEMSTAD, 2000; GOLCHIN et al., 1998; SOLLINS et al., 1996). In most cases organic matter is adsorbed to the surface of the mineral matrix and acts as a bonding agent initiating the formation of a soil aggregate (BALDOCK and SKJEMSTAD, 2000; GOLCHIN et al., 1998; KRULL et al., 2003). Therefore, the more organic matter present in and around the soil particles, the more physically stable the aggregate. This increased stability can, in turn, better protect the organic matter from degradation (BALDOCK and SKJEMSTAD, 2000; GOLCHIN et al., 1998).

Similarly, the organic carbon content of marine continental shelf and slope sediments is intimately linked to the fine-grained, clay-rich sediment fraction (HEDGES

and KEIL, 1995; KEIL et al., 1994; MAYER, 1994a; MAYER, 1994b). Further studies of this association have found that 1) marine sediments are composed of aggregates much like terrestrial soil systems, and 2) organic matter may contribute to the stability of aggregates, thereby acting as a mechanism for long-term organic matter preservation (DAI and BENITEZ-NELSON, 2001; HEDGES and KEIL, 1995; KRULL et al., 2003; MAYER, 1994a; MAYER, 1994b).

This study focuses on the linkages between aggregate size, organic carbon content, and aggregate stability in marine sediments. In particular, we suggest that silt-sized (2-53 μm) aggregates if composed primarily of clay minerals, should be capable of preserving more organic carbon than much smaller clay-sized aggregates (<2 μm). If these silt-size aggregates are also stabilized by organic carbon, they should also have the greatest potential for organic matter preservation.

CHAPTER 2: LITERATURE REVIEW

Organic Carbon in Marine Environments

The primary process of the marine carbon cycle is the formation of organic matter from atmospheric carbon dioxide during the process of photosynthesis. When marine organisms die, the organic matter is either recycled in the water column by heterotrophic organisms or it is removed to the sea floor where benthic organisms recycle a majority of the material (de Haas et al., 2002). Only about 20% of marine organic matter is incorporated into the sediments and sequestered from the marine system (de Haas et al., 2002).

A majority of the organic matter preservation in marine sediments occurs in shelf areas, with a minor component being transported to and preserved in continental slope sediments (Charette et al., 2001; de Haas et al., 2002). Marine shelves, defined as submerged parts of continents, are relatively shallow, with depths generally less than 200 m (de Haas et al., 2002). Although shelves make up <8% of the total ocean surface area, they are responsible for ~45% of the organic matter storage that occurs within the marine environment (de Haas et al., 2002; Hedges and Keil, 1995). For this reason marine shelves are an essential location when examining carbon storage.

ORGANIC CARBON STORAGE AND STABILITY: ROLE OF AGGREGATES

In marine sediments organic carbon can exist as individual particles or it can bond to inorganic minerals (KEIL et al., 1994). Free organic carbon particles are recycled readily and therefore are unlikely to play a large role in long-term carbon storage (KEIL, 2001). By contrast, a strong correlation has been observed between organic carbon content and the concentration of fine-grained, clay mineral particles (HEDGES and OADES, 1997; MAYER, 1994a). Organic matter can associate with inorganic minerals in one of two ways; either (1) adsorption onto mineral grain surfaces, or (2) entrapment within sediment aggregates.

The first hypothesis suggests that organic carbon adsorbs on the surface of minerals (KEIL et al., 1994) either as a monolayer coating of organic compounds adsorbed to the surfaces of inorganic minerals or is embedded within indentions and surface roughness features of mineral grains. For ease of modeling, it is generally assumed that embedded organic carbon occurs in quantities that equal a monolayer coating (Monolayer Equivalent Theory; KEIL et al., 1994; MAYER, 1994b). Use of scanning and transmission electron microscopy (SEM and TEM) however, suggest that organic carbon adsorption is more complex (HULBERT et al., 2002; RANSOM et al., 1997). TEM examination of samples collected off northern California's continental shelf, reveals that organic matter adsorbs as (1) discrete, discontinuous blobs, (2) as bacterial cells and associated muco-polysaccharide networks, and (3) as localized, irregular smears associated with clay mineral and clay rich aggregates (RANSOM et al., 1997). Similarly, scanning electron microscopy (SEM) of marine shelf sediment from the Louisiana Bayou

showed that organic matter can fully encapsulate the mineral surfaces, yet is not uniformly spread over grain surfaces (Figure 2.1; HULBERT et al., 2002). Irregularity of organic carbon coating suggests that although organic carbon adsorption to the surface of inorganic mineral grains occurs, it may not be bound to the grains in a way that would enhance long-term organic matter preservation (BENNETT et al., 1999; HULBERT et al., 2002; RANSOM et al., 1997).

The second hypothesis suggests that organic matter associates with inorganic minerals to form aggregates. A marine aggregate is defined as a cluster of inorganic and organic material that can range from clay-sized (<2 μm) to sand-sized (>63 μm) (KEIL et al., 1994; MAYER, 1994a; MAYER, 1994b; MAYER et al., 2004). It has been speculated that aggregates physically protect organic matter from degradation, thereby promoting its sequestration in marine sediments (HEDGES and OADES, 1997; KRULL et al., 2003; MAYER et al., 2004). Furthermore, individual aggregates can both exist in isolation and bond together to form larger aggregates (Figure 2.2; MAYER et al., 2004; RANSOM et al., 1997). These complex aggregates show an open structure and high porosity throughout their structure (Figure 2.3; HULBERT et al., 2002). The structure of these complex aggregates suggests that organic carbon may act as the bonding agent between inorganic particles or smaller aggregates (MAYER et al., 2004). If this hypothesis is correct, then aggregate stability might be directly correlated with organic carbon content of the aggregate.

To better understand the ability of marine aggregates to preserve organic carbon, Mayer (1994a) examined the ratio between organic carbon and specific surface area of marine aggregates. In sediments between the sediment-water interface and 75 m of

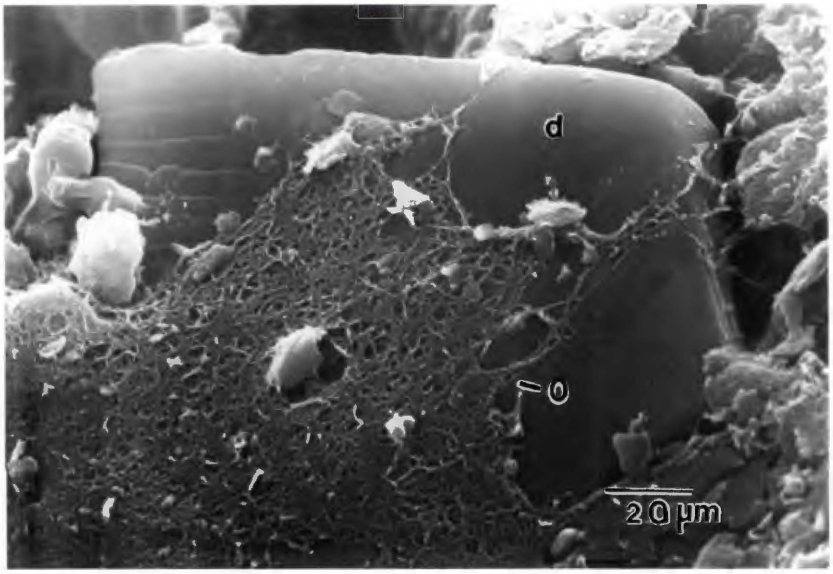

Figure 2.1: SEM of Louisiana Bayou sediment showing drape of organic matter (O) across multiple mineral grains (d) (HULBERT et al., 2002).

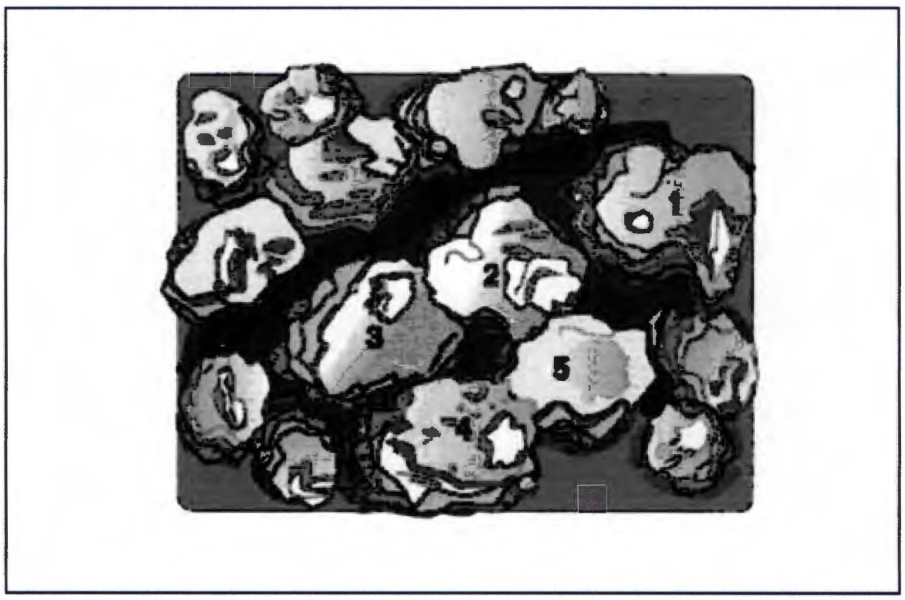

Figure 2.2: Diagram of multi-component aggregates. The numbers indicate individual aggregates bonding together to form a larger aggregate (HULBERT et al., 2002).

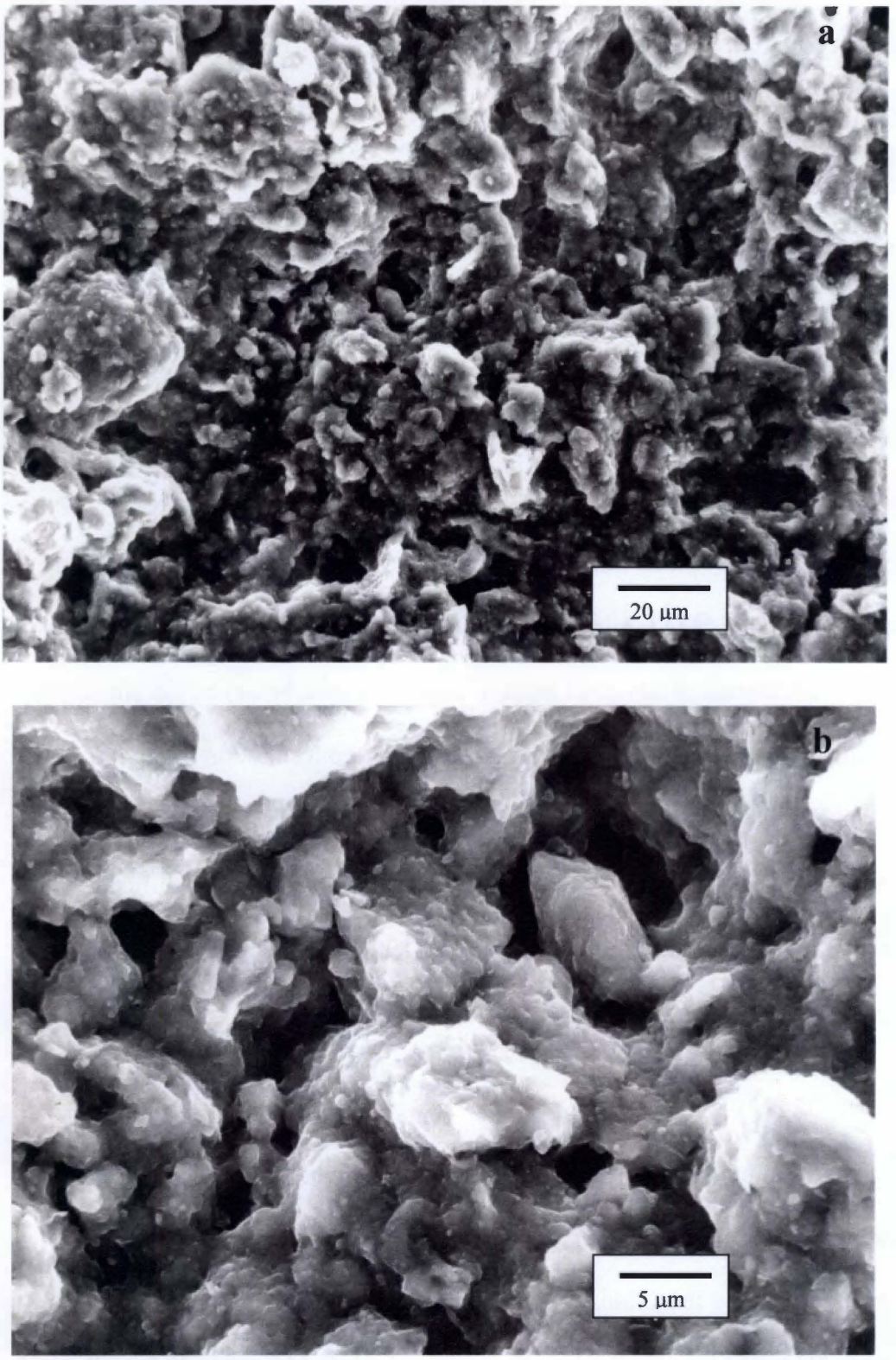

Figure 2.3. Micrographs obtained with an environmental SEM from Louisiana Bayou showing the high porosity and openness of structure a) 20 µm scale b) 5 µm scale (HULBERT et al., 2002).

depth, the concentration of organic matter typically increased as specific surface area of the sediment increased (KAHLE et al., 2002; MAYER, 1994a; MAYER, 1994b; RANSOM et al., 1998) This relationship is typically expressed as a ratio of organic carbon to specific surface area (OC:SFA). Values generally range from 0.2 mg OC m^{-2} to 1.2 mg OC/m^{-2} (HEDGES and KEIL, 1995; MAYER, 1994a).

Interestingly in a study of the aggregate size dependency of OC:SFA, by Keil et. al. (1994) the silt-size fractions (2-53 μm) showed high OC:SFA values , whereas the clay fraction (<2 μm) had low OC:SFA values. They concluded that the lower OC:SFA ratio observed for the clay-sized fraction was likely attributed to a greater surface area of the mineral grains. This greater mineral surface area, however, should have also allowed for a greater concentration of adsorbed organic carbon. It was, however, the silt-sized range, with the higher OC:SFA ratio, that had the highest concentration of organic matter. These data led Keil et al. (1994) to suggest that objects in the silt-sized range, may represent aggregates composed of clay-size grains, which could harbor significantly higher concentrations of organic matter (KEIL et al., 1994).

OBJECTIVE OF THIS STUDY

The observation that silt-size fractions can have a higher organic carbon concentration suggests, first, that silt-size aggregates are composed of clay-sized particles, and second, that the silt-size fraction may have the potential to protect more organic carbon than clay-size fractions (KEIL et al., 1994). Furthermore, if there is more organic carbon within the silt-size range, and if organic carbon is what controls aggregate

stability, then aggregates within the silt-size range should be the most physically stable. This study aims to test whether the potential for organic matter preservation is related to the formation of silt-sized aggregates by examining both organic carbon content and stability of marine aggregates. It was hypothesized that silt-sized aggregates are capable of containing double to triple the amount of organic carbon as clay aggregates and can therefore withstand more physical disturbance. This hypothesis was tested on sediments collected from the Gulf of Maine by separating silt-size particles, silt-size aggregates, clay-size particles, and clay-size aggregates from the bulk sediment and determining systematic differences in the amount of organic matter and aggregate stability.

CHAPTER 3: SAMPLE COLLECTION AND METHODS

SAMPLE COLLECTION

Wilkinson Basin, along with adjacent Jordan and Georges basin are the primary geomorphic depressions of the Gulf of Maine. They were formed during the Pleistocene by glacial plucking and scouring (CONKLING, 1995). The primary contribution of sediment to these basins appears to be fluvial bands associated with the glacial erosion of the surrounding landscape (CONKLING, 1995). Marine sediment samples were recovered on August 27, 2005 at 43° 22' 51 N, 69° 53' 07 W at a depth of 162 meters, just north of Wilkinson Basin, Gulf of Maine (Figure 3.1; CONKLING, 1995). Sediment samples were retrieved using a 10 cm diameter multi-corer (MAYER, 1994a). A single core, 16 cm long, was brought to the surface, and cut into seven stratigraphically distributed samples. The first sample was from the sediment-water interface down to a depth of 1 cm. The next five samples were each 2 cm in length, and the last sample was 5 cm long.

OVERVIEW OF METHODS

A variety of methods were used to (1) isolate the marine aggregate fraction from the surrounding particles and (2) determine the stability of the silt-sized aggregate fraction (Figure 3.2). The bulk sediment was sieved to retain the <53 μm size fraction. The sediment samples were then settled to separate the silt- and clay-size fractions.

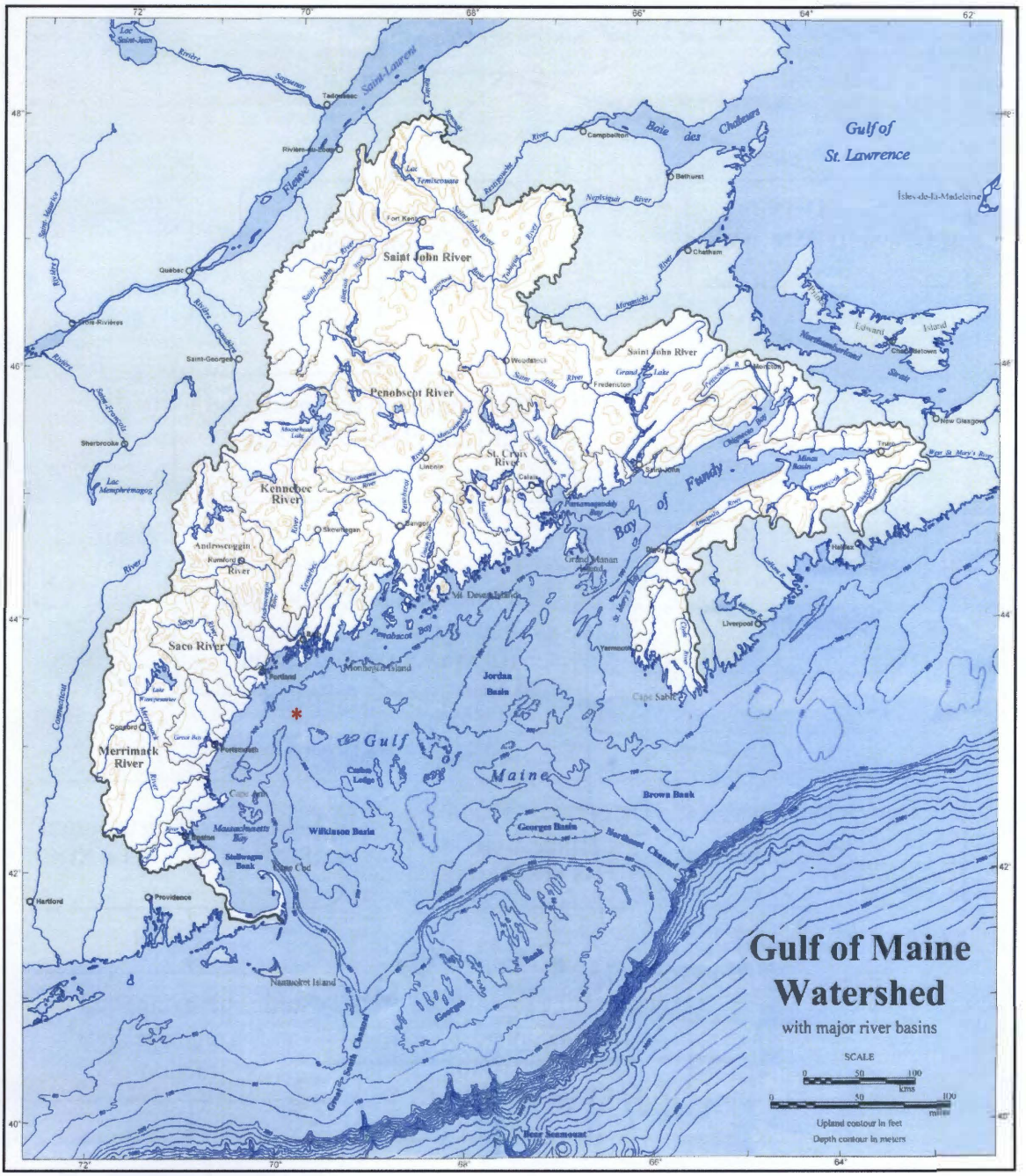

Figure 3.1: Map of Gulf to Maine including watersheds (CONKLING, 1995). The asterisk indicates the location where the sample was collected.

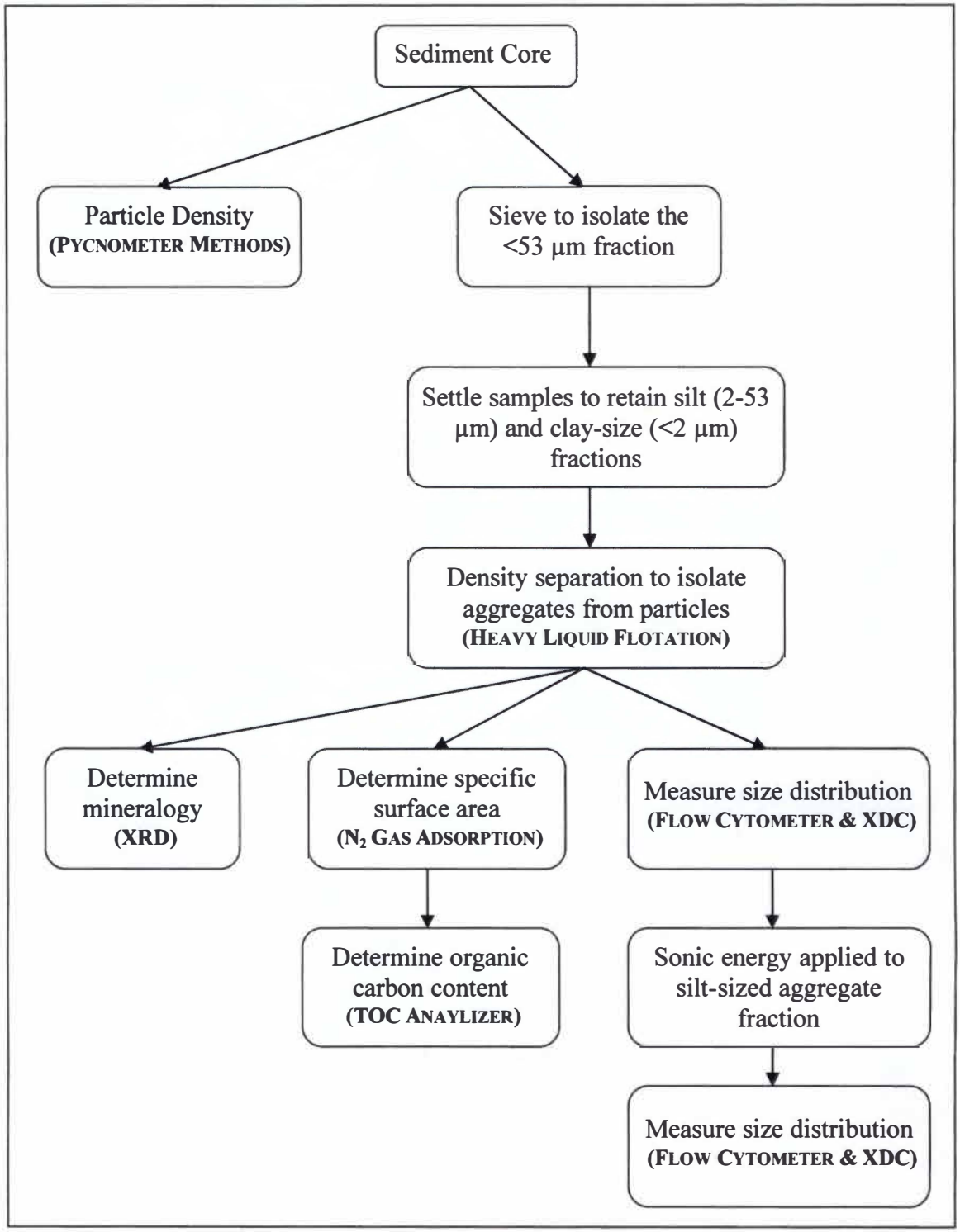

Figure 3.2: Flow chart outlining the steps performed in this study.

A density separation was performed on the different size fractions to isolate the aggregates from the particles. Once this separation process was completed mineralogy was determined and organic carbon content and specific surface area were measured for the silt-sized particle, silt-sized aggregates, clay-sized particles, and clay-sized aggregates fractions. A stability test was then preformed on the remaining sediment sample. A detailed description for each step is outlined below.

PARTICLE DENSITY

The particle density for each sediment sample was measured using the Pycnometer method (KLUTE, 1986). A Pycnometer is a specific-gravity flask fitted with a ground-glass stopper with a capillary opening for a thermometer. In order to remove the effects of pore waters, a subsample of the sediment was washed to remove salt and oven dried to determine water content. 50 grams of sediment was added to a 100 mL pycnometer. The pycnometer with the sediment was then weighed at different temperatures and the values entered into the equation:

$$\rho_p = \rho_w (W_s - W_a) / [(W_s - W_a) - (W_{sw} - W_w)]$$

where

ρ_w = density of water in g cm^{-3} at temperature observed
W_s = weight of pycnometer plus sediment corrected to oven-dry water content
W_a = weight of pycnometer filled with air
W_{sw} = weight of pycnometer filled with sediment and water
W_w = weight of pycnometer filled with water at temperature observed

Particle Size Distribution

Silt- and clay size fractions were separated using a method similar to that outlined by Gee and Bauder (1996). Sediment was sieved to retain the <53 μm size fraction with a seawater solution to prevent flocculation and keep aggregates intact. The seawater solution was mixed to a 2% salt concentration using Aquarium Systems' Instant Ocean (Table 3.1). Sediment from each depth was placed into a 1000 ml graduated cylinder and was filled with deionized water and then 20 mL of the artificial mixed seawater solution was added to prevent flocculation. The cylinders were placed in a constant temperature water bath and allowed to thermally equilibrate. Each column was then stirred and allowed to settle until the silt-size faction of the sediment had settled to the bottom of the column. This process took approximately 22 hours in a constant water temperature of 30 °C. The clay-size fraction in suspension was removed using a vacuum system. The above process was repeated twice to ensure complete removal of the clay-size fraction of the sediment.

Table 3.1: Chemical composition of seawater mixed using Instant Ocean compared to natural seawater. 450 grams of powdered Instant Ocean was added to 3800 mL of deionized water (http://www.aquacraft.net/w0014.html).

Parameter	Instant Ocean (ppm)	Natural Sea Water (ppm)
Chloride	19,154	19,000
Sodium	10,673	10,500
Sulfate	2,684	2,700
Magnesium	1,273	1,350
Calcium	372	400
Potassium	428	380

The clay-size fractions were placed in an oven at 70 ˚C to remove some of the excess water. Once most of the water had been evaporated from the clay-water slurry the samples were put into 50 ml tubes, centrifuged, and decanted to remove the remaining liquid. The silt-size fractions were also placed in 50 ml tubes, centrifuged, and decanted. During this process aliquots were removed to create a sediment size distribution curve according to the method outlined by Gee and Bauder (1996).

Density Fractionation

Heavy liquid flotation is a method that separates objects based on their densities. Organic matter has an average density of 1 g cm^{-1} and sediment particles have a density of approximately 2.6 g cm^{-1} (Bock and Mayer, 2000; Keil, 2001; Keil et al., 1994). If a particle has a significant amount of organic matter adsorbed or incorporated into it, the overall density would lie somewhere between 1-2.3 g cm^{-1}, for marine aggregates; and between 2.3-2.6 g ml^{-1} for individual mineral grains (Bock and Mayer, 2000). A heavy liquid flotation method based on Golchin et al. (1994) was used to differentiate aggregates from individual particles within the separated silt and clay fractions.

The heavy liquid used in this study was sodium polytungstate (NaW), which has a density of 2.3 g ml^{-1}. Approximately 10 g of each silt- and clay-size fraction was placed in centrifugal vials with 25 mL of mixed NaW and homogenized for 30 minutes. Samples were then centrifuged at room temperature at 17,000 rpm for 60 minutes. The supernatant, which consisted of the low-ρ (<2.3 g ml^{-1}) fraction, was removed with a micropipette and rinsed. The vial with the high-ρ fraction (>2.3 g ml^{-1}) pellet, was

refilled with fresh NaW solution and the process was repeated twice more. Once the low-ρ material was removed, the vial containing the remaining high-ρ sediment was filled with distilled water, homogenized, and centrifuged for 15 minutes at 17,000 rpm. At the end of the heavy liquid flotation process it was assumed that the following four fractions had been isolated: silt-sized particles ($\rho>2.3 g\ ml^{-1}$), silt-sized aggregates ($\rho<2.3 g\ ml^{-1}$), clay-sized particles ($\rho>2.3 g\ ml^{-1}$), and clay-sized aggregates ($\rho<2.3 g\ ml^{-1}$).

Mineralogical Composition

Sediment from the silt- and clay-size aggregate fractions were washed with distilled water to remove the crystallized salt, dried, ground, and the mineralogical composition determined using an automated Phillips XRG 3100 X-ray generator by Willamette Geological Service (Moore and Reynolds, 1997). The elemental composition of the bulk sediment was determined using a Phillips MagixPRO wavelength-dispersive X-ray fluorescence (XRF) analyzer (Singer and Janitzky, 1986).

Carbon, Nitrogen, and Specific Surface Area Measurements

The amount of carbon and nitrogen within the four isolated fractions were measured using a procedure outlined by Mayer (1994a). Samples were ground to a fine powder and carbonate removed by vapor-phase acidification. Organic carbon and nitrogen were then analyzed on a Carlo Erba 1106 Elemental Analyzer.

Surface area measurements for each of the four fractions were based on the multi-point BET nitrogen gas absorption method (Bock and Mayer, 2000; Gregg and Sing,

1982). Approximately 1 g of rinsed sample was freeze-dried and then analyzed on a Quantachrome Autosorb-1 Analyzer to obtain the surface area measurements before carbon removal. The samples were then combusted at 550° C for one hour to remove the organic carbon. The samples were then re-analyzed to determine the surface area after carbon removal.

Aggregate Size Distribution and Stability

To determine the difference in the physical stability of silt-sized aggregates, size distribution was determined both before and after sonically disrupting the sample. Both silt- and clay-sized aggregates were measured initially to obtain their original size distributions. Only the silt-sized aggregates were disrupted and remeasured because there was not enough of the clay-sized aggregate fraction to accurately measure the size distribution.

Because sample amount was limited within the silt-size aggregate fraction two different methods were used to measure particle size distrbution. The first method employed a FACSortTM flow cytometer. Approximately 0.5 mL silt- and clay-sized aggregates samples were diluted with an artificial seawater solution to a concentration of 1 parts per million (ppm) and then injected into the flow cytometer with a 100 μm nozzle as outlined by Chernyshev et al. (1995). Flow cytometry utilizes a focused light beam directed through the sample, resulting in forward scattered light (FSC), which is proportional to the size of the particle (Chernyshev et al., 1995). Because flow cytometry can only determine the relative size of the particle relative to the smallest

object detected, it only allows for a qualitative comparison between samples. Quantification of the data is determined by compartmentalizing the data into seven regions, with each successive region having slightly larger particles then the preceding region; region 1 encompassed the smallest sized objects and region 7 had the largest objects. The number of objects within each region was counted and the percent of the total 10,000 objects measured was calculated.

The second method used to measure size distribution utilized a Brookhaven Instruments X-ray Disk Centrifuge (XDC) (STAIGER et al., 2002). This method utilizes the attenuation of X-ray beams passing though a slurry of deionized water and sediment that is being accelerated in a centrifuge, and is capable of measuring very fine particles ($\geq$0.01 μm). Salt water was not used for this portion of the experiment because it was unknown how the dissolved salts would affect the XDCs readings. Deionized water was substituted for salt water. There are only trace amounts of the mineral smectite found in these sediments (MAYER 1994a). The relative absence of expandable clays allows for replacement of salt water for deionized without worrying about major aggregate disruption.

After the size distribution of the silt- and clay-sized aggregate fractions was determined the samples were subjected to sonic disaggregation using a Branson Digital Sonifier. All silt samples were sonicated at using 60 W of power for different lengths of time (GREGORICH et al., 1989), and the amount of energy introduced into the solution was calculated using the equation:

Sonic Energy (J) = (60W)(t) / Sv

where

t = length of time ultrasonic energy applied, (seconds)

Sv = volume of the solution , (mL)

In order to determine how much energy was needed to completely disaggregate the aggregates within the silt-size fraction different amount of energy were applied. Because the amount of sample was limited, only the three samples with the most amount of material were used. The 11-16 cm sample was sonicated with 600 J of energy; 5-7 cm sample was disrupted with 1000 J/mL of energy, and the 7-9 sample was sonicated with 2000 J/mL of energy. Once it was determined that 2000 J/mL of energy was need to completely break apart the aggregates the remaining samples were sonicated with 2000 J/mL of energy.

CHAPTER 4: RESULTS

PARTICLE DENSITY

Raw data for the particle density is found in Appendix A. Table 4.1 lists the calculated particle density for the different depths of the core. A p-value of 0.123 was calculated suggesting that the decreasing trend with depth was not statistically significant. Based on this data the particle density for the entire depth profile was averaged, giving a value of approximately 2.69 g mg^{-1}. This particle density is consistent with other studies (KEIL et al., 1994, MAYER 1994a, BOCK AND MAYER, 2000).

PARTICLE SIZE DISTRIBUTION

Figure 4.1 is a cumulative percent graph depicting the particle size distribution of the sediment after initial sieving (<53 μm) but before sediment was separated into size fractions. A majority of the seven sediment samples (~90%) consist of silt-sized objects (2-53 μm), with only a small portion (~10%) composed clay-sized objects (<2 μm).

Table 4.1: Particle density calculated using the Pycnometer method.

Depth (cm)	Particle Density
0-3	2.764
3-5	2.751
5-7	2.659
7-9	2.636
9-11	2.676
11-16	2.680

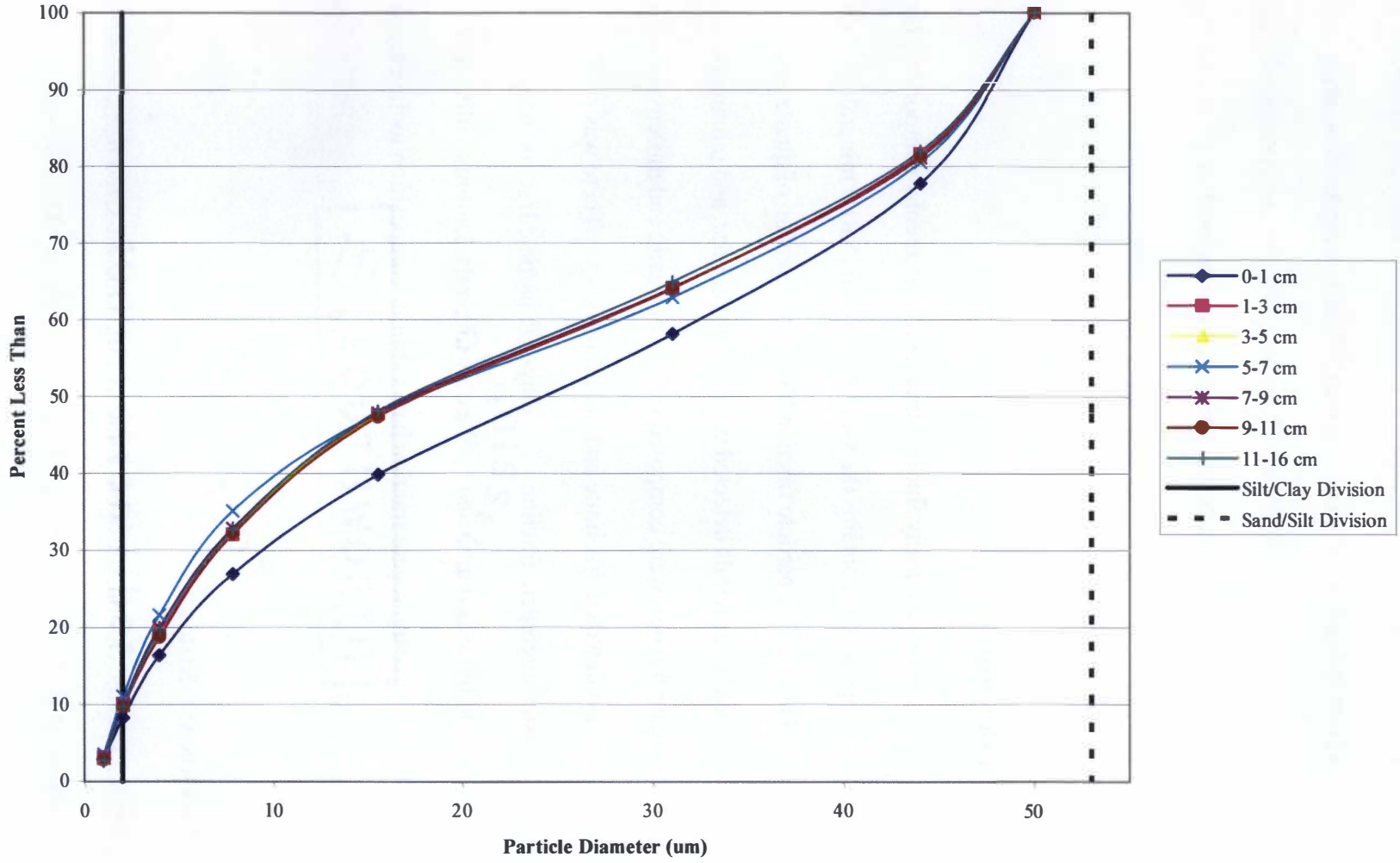

Figure 4.1: Cumulative percent of the particle size distribution for all seven sediment samples.

Samples from different depths tend to follow the same general size trend except for the sample collected from the sediment-water interface, which is composed of larger particles than the remaining six samples. 50% of the 0-1 cm sample collected is composed of objects <23 μm, while 50% of the six deeper samples are composed of objects <17 μm in size.

Mineralogical Composition

Appendix B contains the x-ray fluorescence (XRF) elemental components for the bulk sediment and Appendix C contains the x-ray diffraction (XRD) mineralogy data for the four fractions. The silt-size particle fraction has a large portion of quartz and muscovite. The three clay minerals detected were kaolinite, illite, and montmorillonite. The silt-size aggregate fraction were composed mainly of quartz and muscovite, with only two clay minerals detected; kaolinite and montmorillonite. There was no illite detected in the silt-size aggregate fraction. The clay-size particle fraction had minor amounts of muscovite but was dominated by the clay minerals, kaolinite, illite, and vermiculite. The clay-size aggregate fraction had a similar composition to the clay-size particles but only traces of montmorillonite were detected.

Organic Carbon and Nitrogen

Table 4.2 lists the carbon, nitrogen, and C:N ratios for silt-sized particle, silt-sized aggregate, clay-sized particle, and clay-sized aggregate fraction. The clay-size fraction has the highest organic carbon content with a range of 23.90-61.90 mg g^{-1} and an average

Table 4.2: Organic carbon, nitrogen, and C:N ratios for silt-size particles, silt-size aggregates, clay-size particles, and clay-size aggregates.

	Depth Down Core (cm)	Mean OC (mg/g)	Mean N (mg/g)	C:N		Depth Down Core (cm)	Mean OC (mg/g)	Mean N (mg/g)	C:N
SILT PARTICLES	0	11.45	1.79	6.41	SILT AGGREGATES	0	39.06	3.50	11.18
	1	15.70	2.34	6.71		1	25.83	2.61	9.90
	3	14.84	2.27	6.55		3	23.82	2.48	9.60
	5	6.73	1.25	5.38		5	33.14	3.70	8.97
	7	7.47	1.43	5.24		7	21.64	2.55	8.50
	9	10.20	1.72	5.95		9	14.54	1.49	9.79
	11	6.31	1.28	4.93		11	10.20	1.08	9.44
	AVERAGE	**10.38**	**1.72**	**5.88**		**AVERAGE**	**24.03**	**2.48**	**9.63**
	p-value•	***0.08***	***0.11***	***0.03***		***p-value•***	***0.08***	***0.14***	***0.20***
CLAY PARTICLES	0	13.07	2.01	6.50	CLAY AGGREGATES	0	61.90	6.66	9.29
	1	13.63	2.10	6.49		1	47.54	5.78	8.22
	3	11.27	1.71	6.59		3	58.14	6.58	8.84
	5	12.99	2.19	5.94		5	23.90	3.30	7.24
	7	12.37	2.06	6.00		7	32.82	4.55	7.21
	9	9.94	1.79	5.57		9	47.62	5.52	8.63
	11	*	*	*		11	*	*	*
	AVERAGE	**12.21**	**1.98**	**6.18**		**AVERAGE**	**45.32**	**5.40**	**8.24**
	p-value•	***0.12***	***0.67***	***0.01***		***p-value•***	***0.29***	***0.30***	***0.36***

* Indicates not enough sample to process.

• p-value is for regression significance of variable versus depth.

carbon concentration of 45.32 mg g^{-1}. The next highest organic carbon content was measured in the silt-size aggregate fraction ranging from 10.20-39.06 mg g^{-1} with an average carbon content of 24.03 mg g^{-1}. The silt- and clay-size particle fraction had organic carbon content ranging from 6.31-15.7 mg g^{-1} with and average content of 11.30 mg g^{-1}. In order to determine if there was a trend with depth a regression line was added and the statistical significance was calculated for the four fractions. The p-values are not statistically significant suggesting that there is no correlation between depth and organic carbon.

Nitrogen contents for the silt- and clay-sized particles range from1.25-2.27 mg g^{-1} with an average content of 1.85 mg g^{-1}. The silt-size aggregate fraction ranges from 1.08-3.50 mg g^{-1} with an average of 2.48 mg g^{-1}. The clay-sized aggregate fraction has the highest nitrogen content ranging from 3.30-6.66 mg g^{-1} with an average content of 5.4 mg g^{-1}. The p-values suggest that there is no trend with depth.

The C:N ratios for the silt-sized particles, silt-sized aggregates, clay-sized particles, and clay-sized aggregates are all <10 suggesting that the organic carbon in the these four fractions is from an algal source and not from the terrestrial input of organic matter. The p-values for the silt- and clay-sized aggregate fraction suggested that there is not trend with depth, but the there might be a slight trend with depth occurring in the silt- and clay-sized particle fractions.

Table 4.3: Specific surface area measurements for silt-size particles, silt-size aggregates, clay-size particles, and clay-size aggregates.

	Depth Down Core from Surface Water Interface (cm)	Surface Area with OC (m2/g)	Surface Area with OC Removed (m2/g)	Surface Area Increase with OC Removed (m2/g)	OC:SFA
SILT PARTICLES	0	11.34	13.22	1.88	0.87
	1	15.00	16.82	1.82	1.05
	3	14.38	16.80	2.42	0.88
	5	3.76	4.59	0.83	1.47
	7	5.58	4.69	-0.89	1.59
	9	7.23	8.87	1.64	1.15
	11	4.67	4.82	0.15	1.31
	AVERAGE	**9.11**	**9.71**	**3.00**	**1.19**
CLAY PARTICLES	0	4.88	5.82	0.94	2.24
	1	3.30	4.34	1.04	3.14
	3	1.62	2.24	0.62	5.03
	5	1.81	2.50	0.69	5.19
	7	2.65	3.56	0.91	3.47
	9	1.71	2.15	0.44	4.62
	11	*	*	*	*
	AVERAGE	**2.66**	**3.44**	**0.77**	**3.95**

	Depth Down Core from Surface Water Interface (cm)	Surface Area with OC (m2/g)	Surface Area with OC Removed (m2/g)	Surface Area Increase with OC Removed (m2/g)	OC:SFA
SILT AGGREGATES	0	25.05	*	*	*
	1	6.34	7.17	0.83	3.60
	3	5.04	16.00	10.96	1.53
	5	12.30	16.34	4.04	2.03
	7	5.23	6.86	1.63	3.15
	9	2.70	4.36	1.66	3.33
	11	2.51	3.96	1.45	2.58
	AVERAGE	**8.45**	**9.12**	**4.27**	**2.70**
CLAY AGGREGATES	0	*	5.82	*	10.63
	1	*	4.34	*	10.95
	3	*	2.24	*	25.95
	5	*	2.50	*	9.56
	7	*	3.56	*	9.22
	9	*	2.15	*	22.15
	11	*	*	*	*
	AVERAGE	*	**3.44**	*	**14.74**

* Indicates not enough sample to process.

Surface Area Measurements

Table 4.3 lists the specific surface area data for the four sediment fractions. The highest surface area measurements occurred in the upper 3 cm of depth. Surface area measurements for the silt-size particles, silt-size aggregates and clay-size particles increased when the organic carbon was removed. This relationship has been seen in previous studies and is consistent with a study that suggested small pores are blocked by organic carbon and are exposed with organic carbon removal (Keil et al., 1994; Mayer, 1994a). There was one exception which occurred with the silt-size particle sample taken from 7-9 cm, which showed a surface area decrease when organic carbon was removed. This may be due to the dissolution of roughness elements on the mineral surface or instrumentation error.

There was not enough material to obtain surface area measurements for the clay-size aggregates. A paired T-test was performed between the silt-size particles and silt-size aggregates to determine if the difference in the specific surface area with the organic carbon removed was significant. A p-value of 0.449 was calculated for the paired silt-size particles/silt-size aggregates suggesting that the surface area measurements between the two are statistically similar (Table 4.4). Based on this data the surface area measurements for the clay-size particles were substituted for the missing clay-size aggregate data. The p-values for OC:SFA measurements indicated that there is a statistical difference between silt-size particles and silt-size aggregates. This pattern is repeated between silt particles and clay particles, silt aggregates and clay aggregates, and

Table 4.4: Paired T-test results between fractions and (1) surface area measurements before and after organic matter removal, (2) surface area measurements with organic carbon removed, and (3) OC:SFA. SP=silt-size particle, SA=silt-size aggregates, CP=clay-size particle, and CA=clay-size aggregate. b is SFA before OC removal and a is SFA after OC removal.

Pairs	SFA Before and After OC Removal		Pairs	SFA OC Removed		OC:SFA	
	p-value	Meaning		p-value	Meaning	p-value	Meaning
SPb-SPa	0.0415	Not Similar	SP-SA	0.449	Similar	0.0037	Not Similar
SAb-SAa	0.0377	Not Similar	SP-CP	0.01	Not Similar	0.0009	Not Similar
CPb-CPa	0.0002	Not Similar	SA-CA	*	*	0.0128	Not Similar
CAb-CAa	*	*	CP-CA	*	*	0.0057	Not Similar

* Indicates not enough sample to process.

between clay particles and clay aggregates. This implies that all of the four fractions are statistically different from each other in terms of OC:SFA.

This difference is illustrated in Figure 4.2, which shows the relationship between organic carbon and surface area measurements with the organic matter removed for silt-size particles, silt-size aggregates, clay-size aggregates, and clay-size particles. The silt-size particles have a linear relationship with a moderate variation in surface area measurements (5-17 $m^2 g^{-1}$) and an organic carbon range from 7-16 mg g^{-1}. The silt-size aggregates have the same surface area variability as the silt-size particles but have higher organic carbon concentrations (10-35 mg g^{-1}). The clay-size particles are clustered between 10-15 mg g^{-1} of organic carbon and have small variability in surface area measurements (3-7 $m^2 g^{-1}$). The clay aggregates have the same organic carbon concentrations (20-61 mg g^{-1}) and have small variability in surface area measurements (3-7 $m^2 g^{-1}$). The regression lines for the four fractions are all statistically significant with p-values <0.05.

Size Distribution Prior to Sonication

The flow cytometer plots and size distribution data can be found in Appendix D and the XDC size distribution data can be found in Appendix E. Due to a lack of sample and the quality of measurement output, a combination of the two methods was used to capture size distribution data. Flow cytometry gave complete measurements on all the samples but could not give an absolute size measurement. The XDC could measure absolute size but it had problems capturing and recording x-rays partway through some of

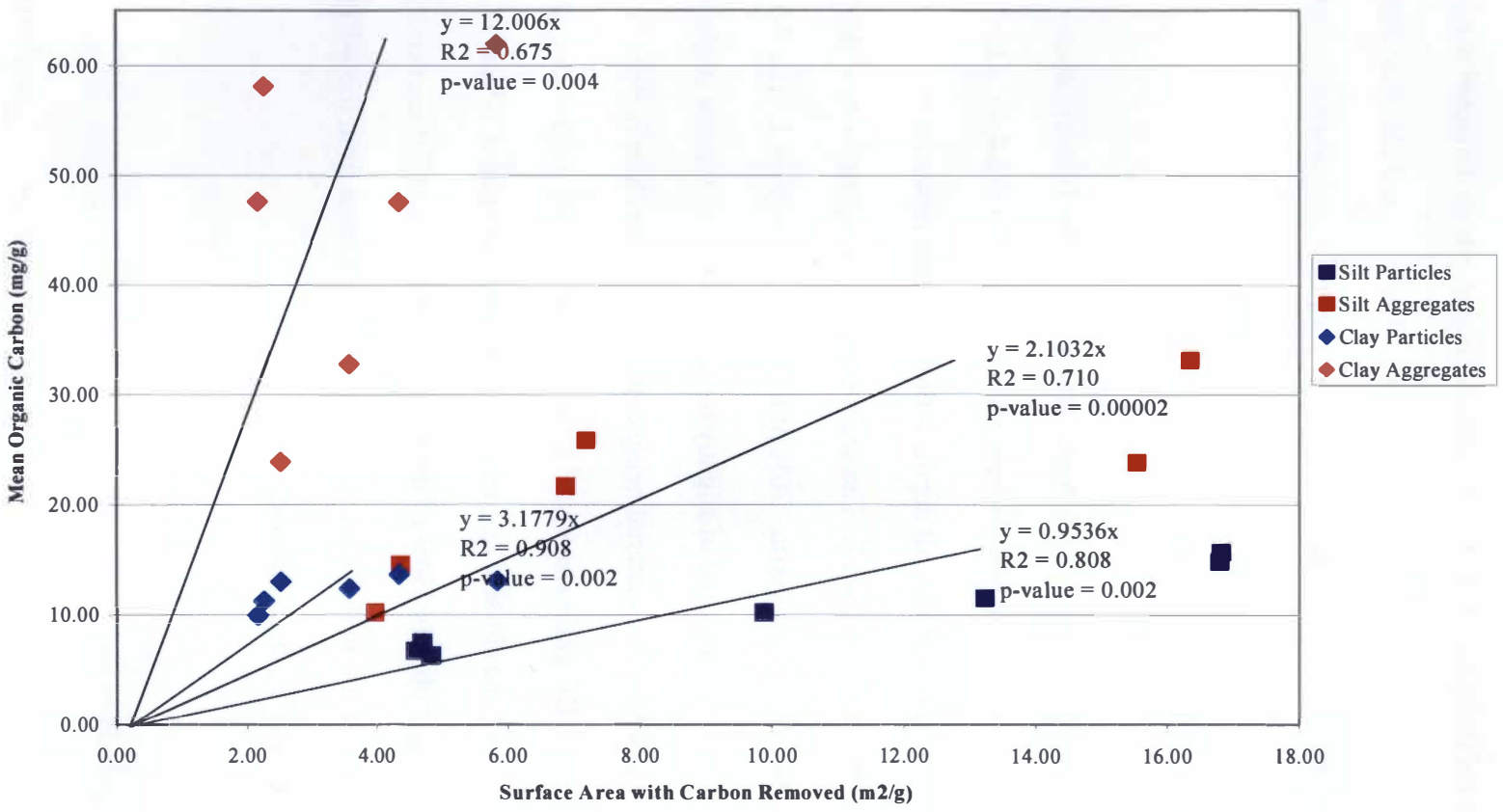

Figure 4.2: Organic carbon and surface area measurements for silt-size particles, silt-size aggregates, clay-size particles, and clay-size aggregates.

the sample runs. This decrease in the quality of size distribution data could be a result of residual sodium polytungstate bound to the mineral grains, which deflected the x-rays. Three samples (0-1 cm, 3-5 cm, and 7-9 cm) from both the silt- and clay-size aggregate fractions gave complete readings and were the only ones used for comparative analysis.

Silt-Size Aggregate Fraction

The size data for the silt-size aggregate fraction from the flow cytometer show little difference in grains size distribution with depth (Figure 4.3 and 4.4). Flow cytometer size distribution data for all depths follow a similar pattern with a majority of their material located within region 1. The sediment from the upper 3 cm of depth is composed of the smallest objects with ~70% of the material in region 1. The 7-9 cm silt-size aggregate fraction is composed of slightly larger objects than the rest of the sediment samples with only ~50% of the material being composed of objects in regions 2-7.

Similarly the XDC grain size distribution data shows little trend with depth (Figure 4.4). However, the silt-size aggregate fraction from a depth of 3-5 cm is composed of the largest objects. 50% of the material from 0-1 and 7-9 cm depths are composed of objects ~1 μm in diameter while 50% of the material from the 3-5 cm depth is composed of objects ~2 μm in diameter.

Clay-Size Aggregate Fraction

All of the seven clay-size aggregate samples have a similar size distribution and the flow cytometry size distribution data showed no trend with depth (Figure 4.5). The

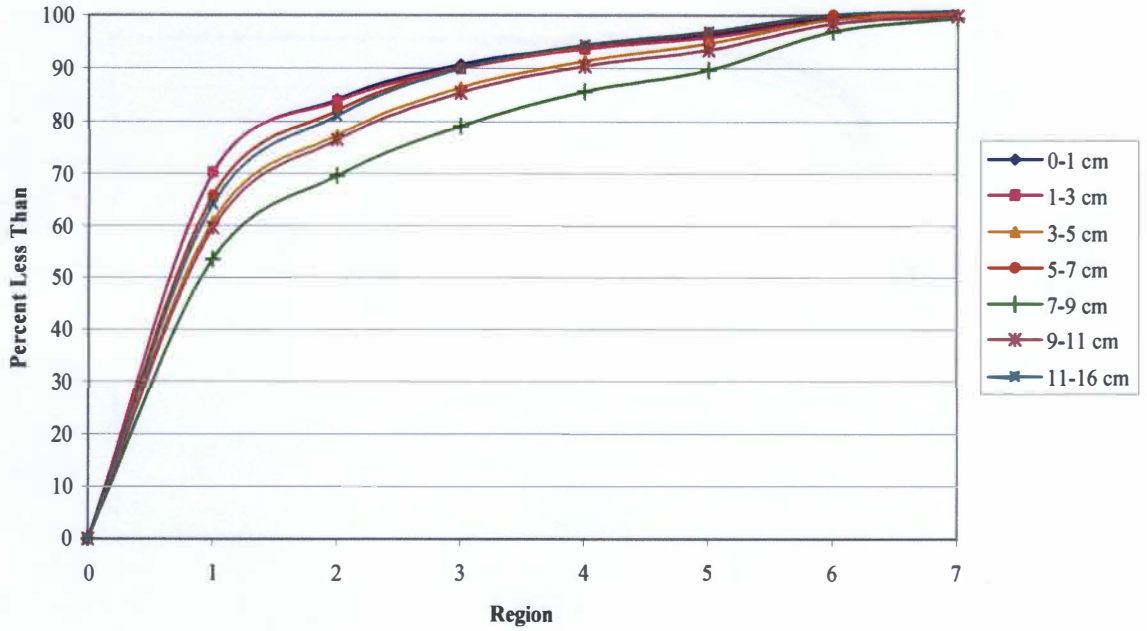

Figure 4.3: Cumulative percent graph for the silt-size aggregate fraction measured with the flow cytometer.

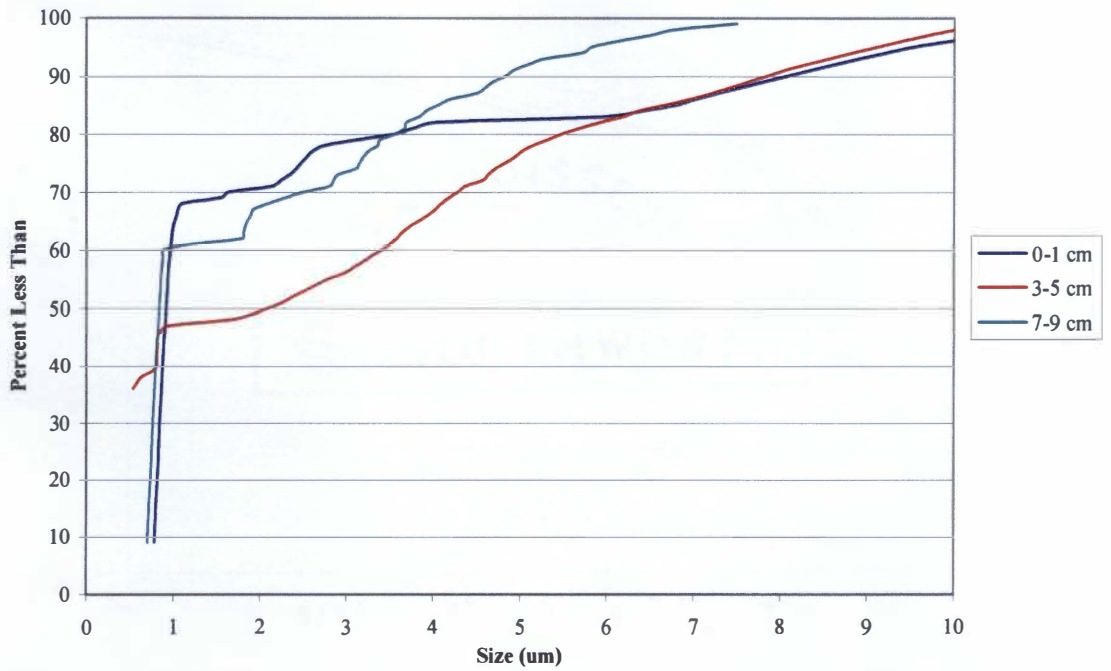

Figure 4.4: Cumulative percent graph forthe silt-size aggregate fraction measured with the XDC.

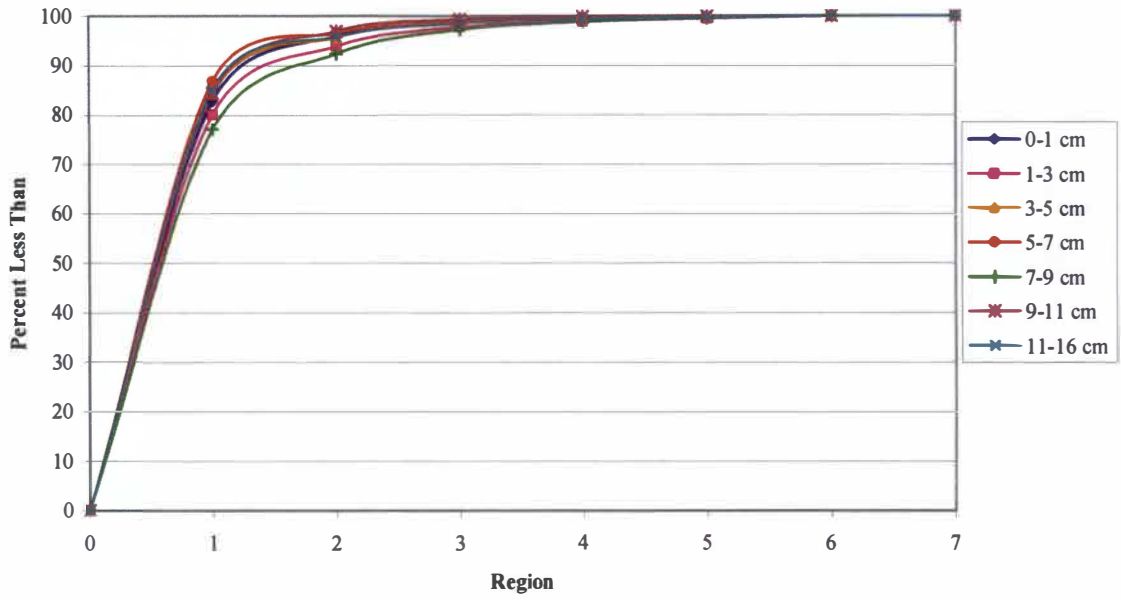

Figure 4.5: Cumulative percent graph for the clay-size aggregate fraction measured with the flow cytometer.

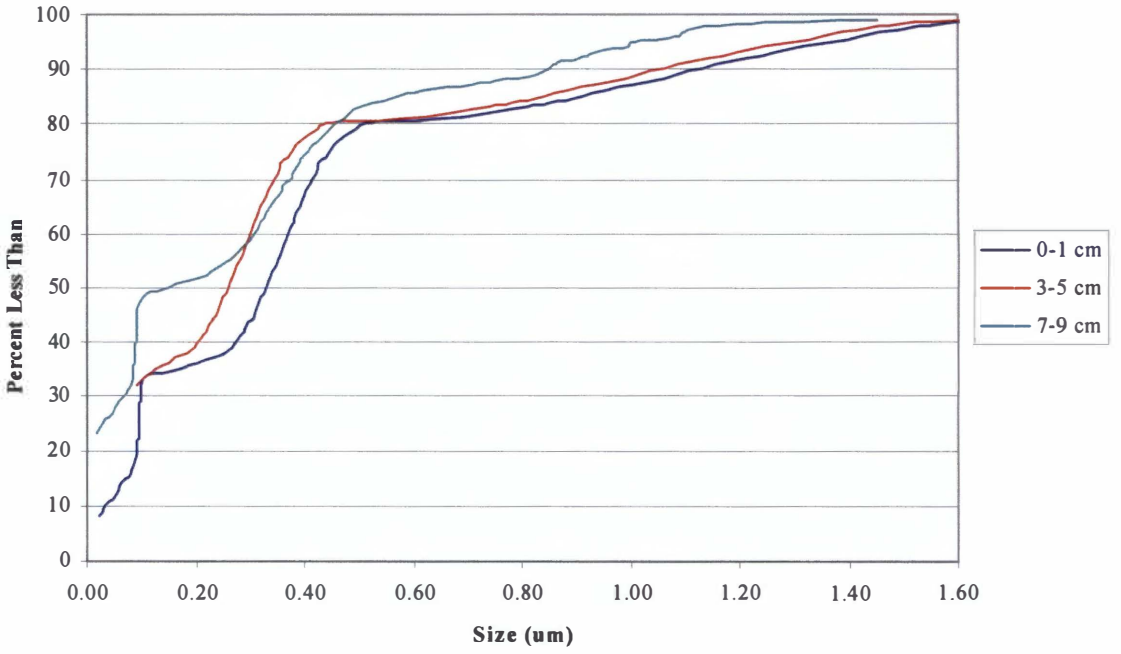

Figure 4.6: Cumulative percent graph for the clay-size aggregate fraction measured with the XDC.

three size distribution curves measured by the XDC suggest a possible trend with depth (Figure 4.6). The deeper sediment sample had more small objects while the shallower sediment sample was composed of larger objects. 50% of the material found at the sediment-water interface was composed of objects ~0.35 μm in diameter. At 3-5 cm of depth 50% of the composition had shifted to ~0.28 μm, and by 7-9 cm 50% of the composition had become even smaller around ~0.18 μm. More data is needed to determine if the observed XDC trend is occurring.

Size Distribution After Sonication

Aggregate Disruption with Increasing Sonic Energy

Once the size distribution of the silt- and clay-size aggregates was determined, the samples were sonicated with increasing energy levels to determine the energy needed to completely disaggregate the aggregate fractions. Only the silt-size aggregate fraction was disrupted with sonic energy because there was not enough material within the clay-size aggregate fraction to get an accurate measurement of aggregate disruption. 600 J/mL, 1000 J/mL, and 2000 J/mL of energy were applied to the silt-size aggregate fraction and the size distribution was measured with the flow cytometer. Only the flow cytometer was used for this step since it required a smaller quantity of sample to obtain an accurate size distribution curve (~0.5 mL of sample for the flow cytometer compared to ~25 mL for the XDC).

Figure 4.7 compares the samples disrupted with increasing levels of sonic energy. The sample sonicated at 600 J was composed of approximately 70.5% small objects

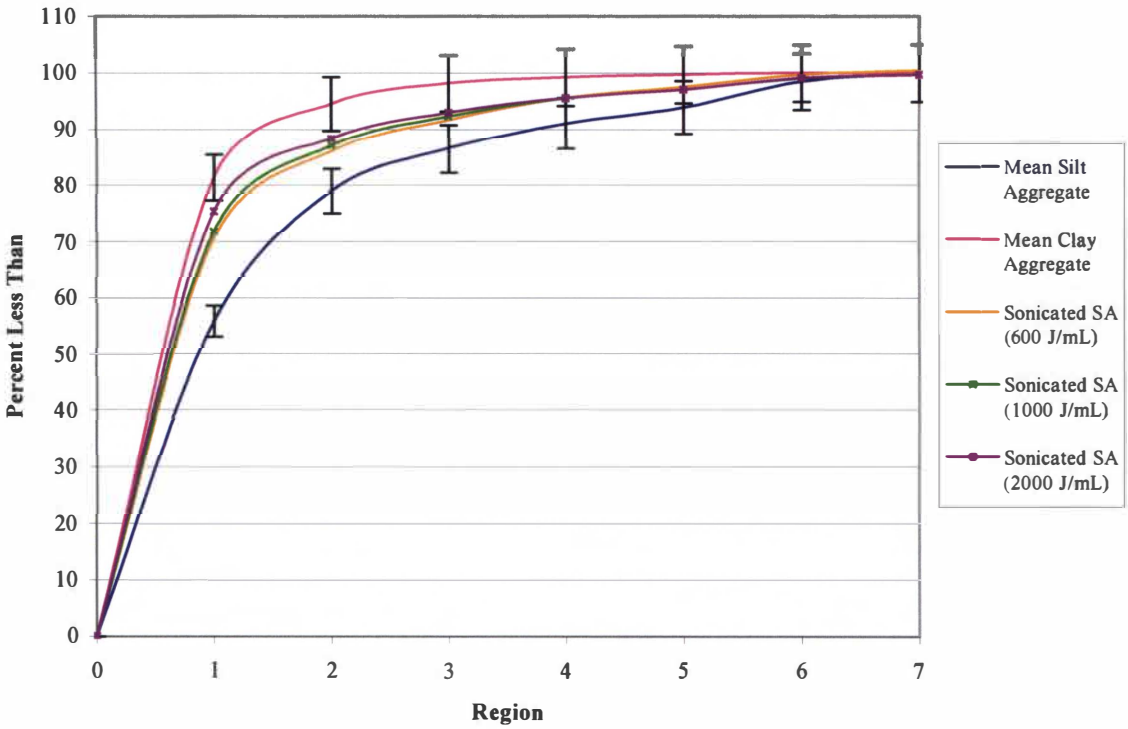

Figure 4.7: Cumulative percent graph created from the flow cytometer data for the silt-size aggregate fraction sonicated with increasing levels of sonic energy. Curves plotted and compared to the non-sonicated silt- and clay-size aggregate fractions. Error bars for 95% confidence level.

(region 1) and 0.7% large objects (region 7). The sample sonicated at 1000 J/mL was composed of approximately 71.8% small objects and 0.7% large objects. The sample with the highest level of sonic energy input, at 2000 J/mL, was composed of approximately 75% small objects and 0.5% large objects. At this point the silt-size aggregates changed from a diverse sample composed of large and small objects (Figure 4.1) to a sample composed almost entirely of smaller particles. This suggests that 2000 J/mL of energy is needed to disaggregate the silt-sized aggregate fraction.

Aggregate Disruption with 2000 J/mL of Sonic Energy

2000 J/mL of sonic energy was applied to the remaining silt-size aggregates and the change in size distribution was measured with the flow cytometer and the XDC . The flow cytometer size distribution curves show a slight trend with depth, with the deeper sediment samples having a larger portion of their composition composed of larger particles than the sediment-water interface sample (Figure 4.8). The silt-size aggregate fraction that had been disrupted with 2000 J/mL of sonic energy was measured by the XDC and the equivalent diameter for 50% of the sample composition (d_{50}) was calculated from the size distribution data. Table 4.5 shows the d_{50} for the silt-size aggregates, clay-size aggregates, and silt aggregates sonicated with 2000 J/mL of energy. Measurements from the XDC indicated that before the silt-size aggregates were disrupted the average d_{50} was ~1 μm and after sonication the average d_{50} dropped to ~0.03 μm.

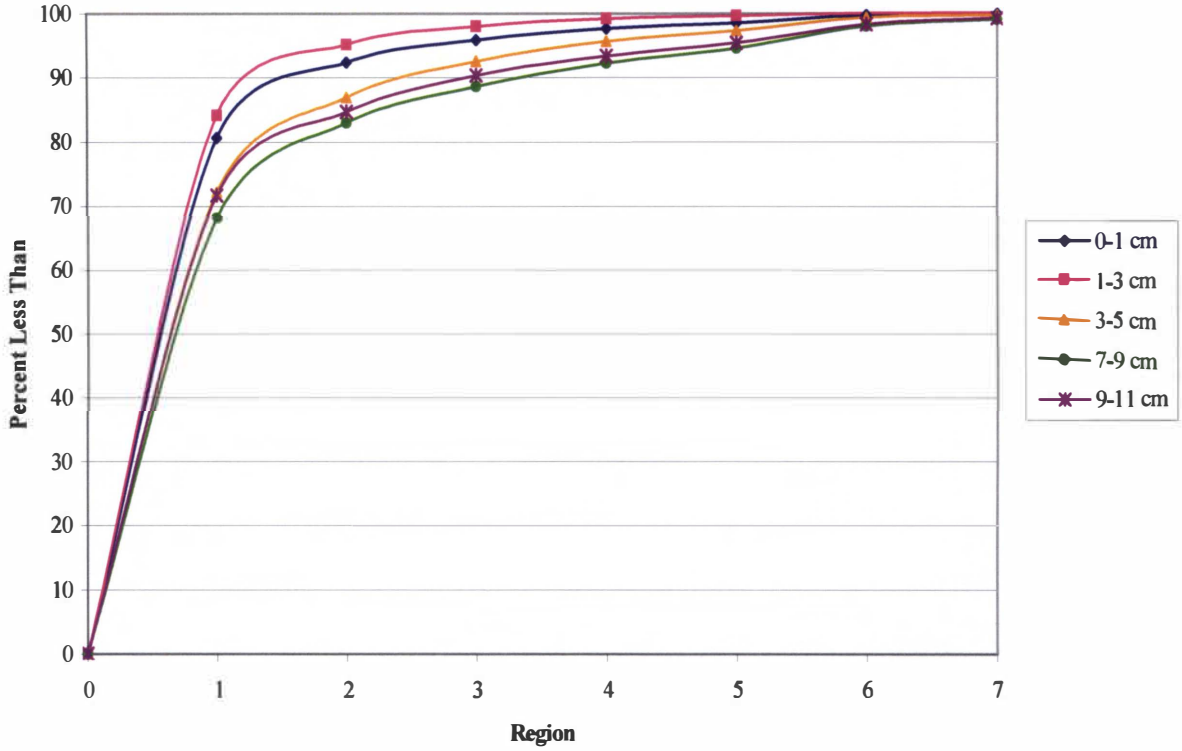

Figure 4.8: Cumulative percent graph created from the flow cytometry data for the silt-size aggregate fraction sonicated with 2000 J/mL of sonic energy

Stability Ratios

In order to determine the effect the 2000 J/mL of sonic energy had on the silt-size aggregate fraction stability ratios were calculated (Table 4.5). To calculate the stability ratio the d_{50} for the sonicated silt-size aggregate fraction was divided by the d_{50} for the initial silt-size aggregate fraction and converted to a percentage. The stability ratios were then plotted against the organic carbon content measured within the silt-size aggregate fraction (Figure 4.9). A regression line was added which suggests that there is no correlation between the amount of organic carbon and the stability of the silt-size aggregate fraction. The stability ratio and organic carbon content were then plotted versus depth (Figure 4.10). Both the stability ratio and organic carbon concentration decrease with depth, but the amount of organic carbon does not appear to be the only mechanism controlling the stability of the aggregate. The sample from 0-1 cm depth has the second lowest stability ratio but it has the most amount of organic carbon. Conversely, the 3-5 cm sample has the highest stability ratio but it only has a moderate amount of organic carbon.

Table 4.5: XDC equivalent diameter (μm) of 50% of the silt-size aggregates, clay-size aggregates, and silt-size aggregate disrupted with 2000 J/mL of sonic energy. Stability ratios are listed for the disrupted silt-size aggregates.

Depth	d_{50}			Stability Ratio (%)	Organic Carbon (mg/g)
	Silt Aggregate	Clay Aggregate	Sonicated Silt Aggregate		
0	0.919	0.33	0.024	2.612	39.06
1	0.356	*	0.027	7.584	25.83
3	0.301	0.017	0.049	16.279	23.82
7	2.097	0.026	0.034	1.621	21.64
9	0.857	0.021	0.031	3.617	14.54

* Indicates not enough sample to process.

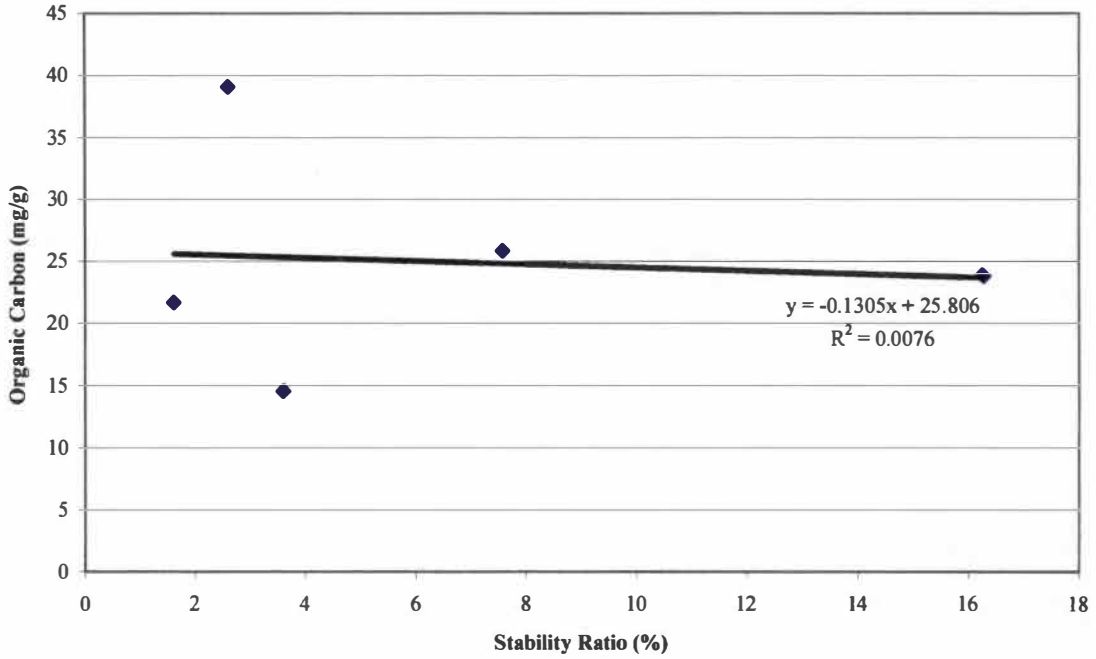

Figure 4.9: Stability ratio versus organic carbon content for the disrupted silt-size aggregate fraction.

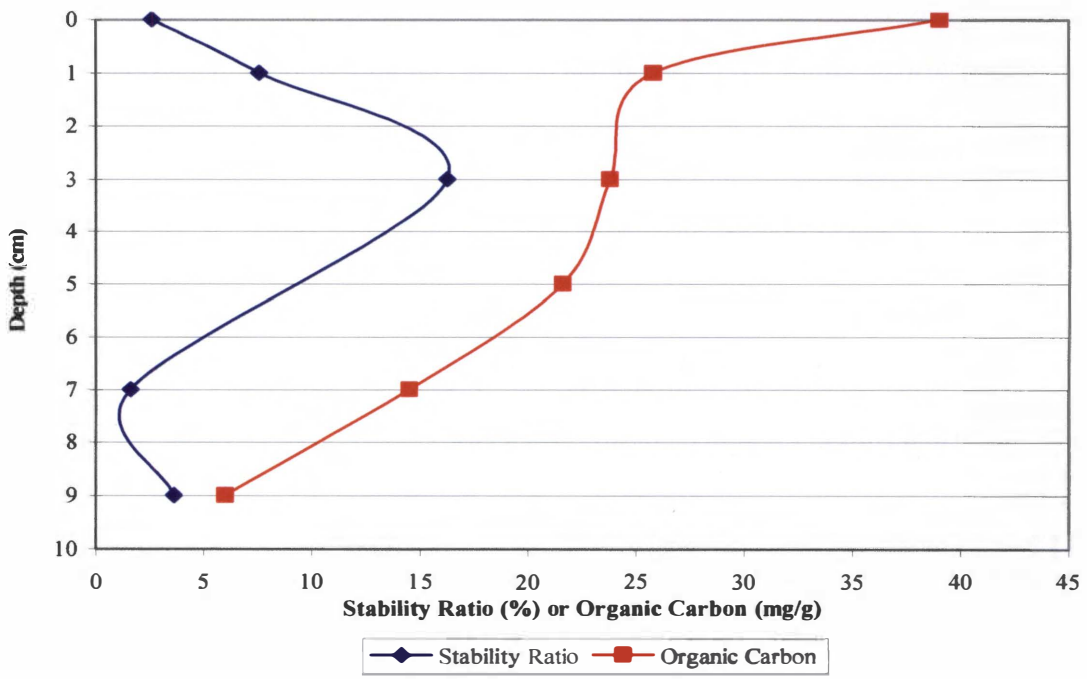

Figure 4.10: Stability ratios for the silt-size aggregates disrupted with 2000 J/mL of sonic energy plotted against organic carbon contents.

CHAPTER 5: INTERPRETATION AND DISCUSSION

MINERALOGY

XRD data detected that the silt-sized fraction is composed predominantly of quartz and muscovite, with lesser amount of the clay minerals, kaolinite and montmorillonite. Kaolinite is a nonexpandable clay and is not prone to shrinking or swelling. Although synthetic sea water was used whenever possible, the presence of nonexpandable clays made the substitution of deionized water not as detrimental to the integrity of the aggregates. Montmorillonite has a small particle size and an extremely large surface area and is susceptible to shrinking and swelling in the presence of deionized water (DIXON and WEED, 1977). The use of deionized water on therefore could have potentially altered the structurally integrity of the aggregates. The clay mineral illite was detected within the silt-size particle fraction, but not in the silt-size aggregate fraction. Smectite, in this case montmorillonite, coverts into illite during the process of diagenesis (NESSE, 2000). The presence of illite could indicate that silt-size particles have undergone more diagenesis than silt-size aggregates, perhaps indicating the protective nature of the aggregates.

The clay-size fraction was dominated by the clay minerals kaolinite, illite, and vermiculite. The absence of montmorillonite in the clay-size particle fraction could suggest that this has undergone diagenesis. The clay-size aggregate fraction did detect some montmorillonite, which could mean that the clay-size aggregate fraction is

undergoing diagenesis but has not converted all of the montmorillonite to illite (NESSE, 2000).

ORGANIC CARBON AND STABILITY

The observation by Keil et al. (1994) that silt-sized components had higher concentrations of organic matter than clay-size components was the foundation for this study. It was speculated that an increase in organic carbon would also make the silt-sized aggregates more physically stable. In this study, when aggregates were isolated from particles, it was observed that clay-sized aggregate fraction had more carbon (45.32 mg g^{-1}) then silt-sized aggregate fraction (24.03 mg g^{-1}) (Table 4.2). These results do not support the first part of the hypothesis and are contrary to those of Keil et al. (1994). These data could suggest potentially more complex organic carbon-aggregate relationships.

There was not enough material within the clay-size aggregate fraction to test their physical stability but some observations about the silt-size aggregate fraction where made. It was determined that at least 2000 J/mL of sonic energy is needed to completely break up silt-size aggregates (Figure 4.7). The trend with depth observed in Figure 4.8 suggests that when the same amount of energy is applied to the silt-size aggregate fraction the samples closer to the sediment-water interface break into small components while deeper samples are able to maintain their larger components. This could be the result of physical process such as compaction, dewatering, and/or lithification beginning to occur around 3 cm of depth.

There was no correlation between the amount of organic carbon and the stability of the silt-sized aggregates (Figure 4.9). In order to examine what might be controlling the relationship between stability and organic carbon, stability ratios were plotted versus depth (Figure 4.10). It was observed that the highest amount of organic carbon occurred at the sediment water interface and had the least stable aggregates. This is to be expected since this area is continually replenished with organic carbon from the water column, and is also subject to physical disturbance from benthic organisms. The most stable silt-size aggregates occurred around 3 cm of depth, with only a moderate amount of organic carbon present. This increased stability could also be the result of the physical process mentioned above or it could result from the quality of organic carbon present. The organic carbon at 3 cm of depth could be changing from transient organic carbon and beginning to be incorporated into the sediment fabric. It could also be that there is an organic carbon threshold, above which the aggregate stability is no longer increased.

Disrupted Aggregates

Two findings of this study suggest that the silt-sized aggregate fraction was disrupted by the aggregate separation methods. The first is the comparison between the size distribution curve created at the beginning of the experiment (Figure 4.1) and the one created after isolating the aggregate fractions (Figure 4.4). During the initial settling process the silt-size aggregate fraction was 2-48 μm in size. When the size distribution was measured again prior to the application of sonic energy the silt-size aggregate fraction was composed of particles 0.4-14 μm in size. Decreases in both the lower and

upper limits of the size distribution indicate that the separation methods employed between initial settling techniques and the application of sonic energy disrupted the silt-size aggregate fraction.

The second finding that suggests that the silt-size aggregate fraction was disrupted is the surface area measurements. The higher surface area measurements for the silt-size particles and aggregates (3.96-16.80 $m^2 g^{-1}$) suggest that the silt-size fraction is partially composed of clay mineral grains. The presence of clay minerals such as kaolinite, illite, and montmorillonite detected by the XRD supports this suggestion. In the Gulf of Maine the dominant clay mineral is kaolinite (MAYER et al., 2004) and if the silt-size aggregate fraction is dominantly composed of clay mineral grains, it would explain why the surface area measurements found in Table 4.3 coincide with the surface area measurements of individual kaolinite particles. Dixon and Weed (1977) used a glycerol adsorption method to determined kaolinite mineral surface areas and measured a range of 5.0-14.5 $m^2 g^{-1}$. Schofield and Samson (1954) recorded surface area measurements of 8-25 $m^2 g^{-1}$ using the negative adsorption method and 6-39 $m^2 g^{-1}$ with the nitrogen BET method. The fact that the surface area measurements were consistent with the surface area of individual kaolinite grains suggests that the silt-size aggregate fraction was disrupted and is no longer composed of aggregates but individual particles.

The disaggregation of the larger aggregates within the silt-size fraction is an indication of their inherent instability. Of the sampling methods applied the heavy liquid flotation had the potential to be very destructive. When the flotation process is employed using the monovalent ion cesium chloride (CsCl) there does not appear to be much organic carbon dissolution (BOCK and MAYER, 2000; KEIL et al., 1994). The problem is

that CsCl is limited to a maximum density of 1.9 g cm^{-3} and studies have shown that this density range does not include many silt- and clay aggregates (BOCK and MAYER, 2000). It has been calculated that marine aggregates have a density of approximately 2.2 g/cm^3 (BOCK and MAYER, 2000). In order to isolate this density range and consequently isolate the aggregates from the surrounding particles the divalent anion sodium polytungstate (NaW) was used. NaW has the potential to cause dissolution of organic matter (BOCK and MAYER, 2000). If some of the organic matter was dissolved, a potential bonding mechanism between the mineral grains could have been removed, resulting in a disrupted aggregate. It is also possible that the force applied to the aggregates during the high speed centrifuge process may have led to disaggregation.

No size distribution data was collected on the clay-size aggregate fraction at the beginning of the experiment. The only measurement made on the clay-size fraction was to determine that ~10% of the sieved sediment was composed of objects <2 μm in diameter (Figure 4.1). After isolating the aggregates from the particles, the XDC detected a size range of 0.35-1.8 μm. The upper limit of 1.8 μm is very close to the initial starting diameter of 2 μm. This could suggest that the clay-size aggregate fraction was not disrupted and maintained its structural integrity but more data is needed to determine if this phenomenon is occurring.

LIMITATIONS OF ANALYTICAL TECHNIQUES

It is important to note some of the problems with this study. Few studies have been conducted on silt- and clay samples gathered from natural marine sediments (KEIL

et al., 1994). This results from the difficulty in retrieving large quantities of sediment within specified size fractions (KEIL et al., 1994). Several methods, such as sieving, settling, centrifugation, and filtration are commonly used for isolating different size fractions from marine sediment but they frequently do not provide enough material to analyze many inorganic and organic components (KEIL et al., 1994). This study revealed these common difficulties. After isolating silt and clay samples from two 16 cm deep sediment cores, there was only enough material in the clay-size range to obtain surface area measurements from six of the fourteen samples. This lack of information could potentially alter the interpretations that can be made pertaining to the clay fraction of the sediment.

A bigger issue is that surface area measurements of clay-sized particle and aggregate fractions were smaller than that of silt-sized particle and aggregate fractions (Table 4.3, Figure 4.2). This should not be true, because spherical shaped quartz grains found in the silt-size fraction, will always have a smaller surface area than a platy mineral grain found in the clay-size fraction (NESSE, 2000). If the silt- and clay-size fractions of the sediment were composed of the same mineral grains then the surface area measurements should be relatively equal or the clay-size fraction should be higher if clay mineral grains dominate sample. The absence of these trends suggests that the surface area measurements are not accurate, at least for the clay-size fraction of the sediment. It could be that there was not enough sample to get an accurate surface area measurement. The machine did die while running the last clay-size particle sample and the low surface area measurements could be an indication that the machine was not working properly prior to its death.

CHAPTER 6: CONCLUSIONS AND FUTURE RESEARCH

The primary finding of this study is that the clay-size aggregate fraction from marine sediments from the Gulf of Maine had the highest carbon content. The higher carbon content measured in the clay-size aggregate fraction may indicate that organic carbon is preferentially associated with smaller mineral grains, specifically clay mineral grains.

Silt-size aggregates may be more stable than clay-size aggregates and may be more capable of preserving organic carbon through time but it is unknown since (1) the silt-size aggregate fraction was disrupted, and (2) there was not enough clay-size aggregate material to test stability. Based on the stability ratios calculated for the silt-size aggregate fraction, the most stable silt-size aggregate occurs around 3 cm of depth, and does not appear to be correlated to the amount of organic matter present. It could be that at this depth organic carbon is changing from transient carbon and is becoming incorporated into the sediment fabric. More information is needed on the relationship between organic carbon and stability of aggregates, especially trends with depth.

More research needs to be conducted on the factors influencing the strength of marine aggregates. Removing the sediment from the marine environment and applying laboratory methods has the possibility to disrupt the structural integrity of the aggregates. Replicate analysis of this study would allow size distribution data to be collected after each step in the aggregate isolation process to determine if any of the steps are destroying the structural integrity of the aggregates. If so, then new methods need to be employed that do not destroy the object under investigation.

REFERENCES

Baldock J. A. and Nelson P. N. (1999) *Soil organic matter*. CRC Press.

Baldock J. A. and Skjemstad J. O. (2000) Role of the soil matrix and minerals in protecting natural organic materials against biological attack. *Organic Geochemistry* **31**, 697-710.

Bennett R. H., Ransom B., Kastner M., Baerwald R. J., Hulbert M. H., Sawyer W. B., Olsen H., and Lambert M. W. (1999) Early diagenesis: Impact of organic matter on mass physical properties and processes, California continental margin. *Marine Geology* **159**, 7-34.

Bock M. J. and Mayer L. M. (2000) Mesodenstiy organo-clay associations in a near-shore sediment. *Marine Geology* **163**, 65-75.

Charette M. A., Moran S. B., and Pike S. M. (2001) Investigating the carbon cycle in the Gulf of Maine using the natural tracer thorium 234. *Journal of geophysical research* **106**, 11553-11579.

Chernyshev A. V., Prots V. I., Doroshkin A. A., and Maltsev V. P. (1995) Measurment of scattering properties of individual particles with a scanning flow cytometer. *Applied Optics* **34**(27), 6301-6305.

Conkling P. W. (1995) *From Cape Cod to the Bay of Fundy - An Environmental Atlas of the Gulf of Maine*. MIT Press.

Dai M. H. and Benitez-Nelson C. R. (2001) Colloidal organic carbon and 234Th in the Gulf of Maine. *Marine Chemistry* **74**, 181-196.

de Haas H., van Weering T. C. E., and de Stigter H. (2002) Organic carbon in shelf seas: sinks or sources, processes and products. *Continental Shelf Research* **22**, 691-717.

Dixon J. B. and Weed S. B. (1977) *Minerals in Soil Environments*. Soil Science Society of America.

Gee G. W. and Bauder J. W. (1996) Particle-size analysis. In *Methods of Scoil Analysis, Part I*, pp. 383-411. American Society of Agronomy--Soil Science Society of America.

Golchin A., Baldock J. A., and Oades J. M. (1998) *A model linking organic matter decomposition, chemistry and aggregate dynamics*. CRC Press.

Golchin A., Oades J. M., Skjemstad J. O., and Clarke P. (1994) Soil structure and carbon cycling. *Australian journal of Soil Research* **32**, 1043-1068.

Gregg S. J. and Sing K. S. W. (1982) *Asorption, Surface Area and Porosity*. Adacemic Press.

Gregorich E. G., Kachanoski R. G., and Voroney R. P. (1989) Carbon mineralization in soil size fractions after various amounts of aggregate disruption. *European Journal of Soil Science* **40**(3), 649.

Hedges J. I. and Keil R. G. (1995) Sedimentary organic matter preservation: An assessment and speculative synthesis. *Marine Chemistry* **49**, 81-115.

Hedges J. I. and Oades J. M. (1997) Comparative organic geochemistries of soils and marine sediments. *Organic Geochemistry* **27**(7/8), 319-361.

Hulbert M. H., Bennett R. H., Baerwald R. J., Long R. L., Curry K. J., L. C. A., and Abril M. T. (2002) Observation of the sediment-water interface: Marine and fresh water environments. *Marine Georesources and Geotechnology* **20**, 255-274.

Kahle M., Kleber M., and Jahn R. (2002) Predicting carbon content in illitic clay fractions from surface area, cation exchange capacity and dithionite-extractable iron. *European Journal of Soil Science* **53**, 639-644.

Keil R. G. (2001) Organic-mineral interactions in marine sediments studied using density fractionation and X-ray photelectron spectroscopy. *Organic Geochemistry* **32**, 1401-1415.

Keil R. G., Tsamakis E., Bor Fuh C., Giddings J. C., and Hedges J. I. (1994) Mineralogical and textural controls on the organic composition of coastal marine sediments: Hydrodynamic separation using SPLITT-fractionation. *Geochimica et Cosmochimica Acta.* **58**, 879-893.

Klute A. (1986) Methods of Soil Analysis Part 1. American Society of Agronomy, Inc.

Krull E. S., Baldock J. A., and Skjemstad J. O. (2003) Importance of mechanisms and processes of the stabilisation of soil organic matter for modelling carbon turnover. *Functional Plant Biology* **30**, 207-222.

Mayer L. M. (1994a) Surface area control of organic carbon accumulation in continental shelf sediments. *Geochimica et Cosmochimica Acta.* **58**, 1271-1284.

Mayer L. M. (1994b) Relationships between mineral surfaces and organic carbon concentrations in soils and sediments. *Chemical Geology* **114**, 347-364.

Mayer L. M., Schick L. L., Hardy K. R., Wagai R., and McCarthy J. (2004) Organic matter in small mesopores in sediments and soils. *Geochimica et Cosmochimica Acta.* **68**, 3863-3872.

Moore D. M. and Reynolds R. C. (1997) *X-Ray diffraction and the identification and analysis of clay minerals.* Oxford University Press.

Nesse W. D. (2000) *Introduction to Mineralogy.* Oxford University Press.

Ransom B., Bennett R. H., Baerwald R. J., and Shea K. (1997) TEM study of in situ organic matter on continental margins: occurrence and the monolayer hypothesis. *Marine Geology* **138**, 1-9.

Ransom B., Kim D., Kastner M., and Wainwright S. (1998) Organic matter preservation on continental slopes: Importance of mineralogy and surface area. *Geochimica et Cosmochimica Acta.* **62**, 1329-1345.

Schofield R. K. and Samson H. R. (1954) Flocculation of kaolinite due to the attraction of oppositely charged crystal faces. *Discussions of the Faraday Society* **18**, 135-145.

Singer M. J. and Janitzky P. (1986) Field and laboratory procedures used in a soil chronosequence study. *United States Geological Survey Bulletin* **1648**, 49.

Sollins P., Homann P., and Caldwell B. A. (1996) Stabilization and destabilization of soil organic matter: mechanisms and controls. *Geoderma* **74**, 65-105.

Staiger M., Bowen P., Ketterer J., and Bohonek J. (2002) Particle Size Distribution Measurement and Assessment of Agglomeration of Commercial Nanosized Ceramic Particles. *Journal of Dispersion Science & Technology* **23**(5), 619.

APPENDICES

APPENDIX A: PYCNOMETER DATA

Particle Density for Gulf of Maine Samples

Depth (cm)	Dry Picnometer	Soil	Pyc + dry soil	Pyc + soil +water 2	Pyc + water
0-3	20.1112	9.1442	29.2554	74.8536	69.8584
3-5	20.1028	9.3718	29.4746	75.0593	69.8263
5-7	22.1613	9.4020	31.5633	77.4018	71.8275
7-9	22.6808	9.1345	31.8153	78.0327	72.3433
9-11	19.7512	9.5160	29.2672	75.3222	69.3990
11-16	25.5704	9.2548	34.8252	80.9771	75.3021

WATER CONTENT

Depth (cm)	wet soil + beaker	dry soil + beaker	beaker	w g/g	w %
0-3	16.5868	16.2979	14.3318	0.1469	14.6941
3-5	16.8080	16.5329	14.3441	0.1257	12.5685
5-7	15.3397	15.1271	11.1395	0.0533	5.3315
7-9	15.7077	15.7074	14.3756	0.0002	0.0225
9-11	14.4278	14.3984	11.3847	0.0098	0.9755
11-16	17.0868	17.0061	13.8090	0.0252	2.5242

Depth (cm)	Ws	Wa	Wsw	Ww	rho w
0-3	27.9117	20.1112	74.8536	69.8584	2.7637
3-5	28.2967	20.1028	75.0593	69.8263	2.7505
5-7	31.0620	22.1613	77.4018	71.8275	2.6595
7-9	31.8132	22.6808	78.0327	72.3433	2.6363
9-11	29.1744	19.7512	75.3222	69.3990	2.6760
11-16	34.5916	25.5704	80.9771	75.3021	2.6796

* *water density =0.9939154*

Statistical Measurements on the particle density

Mean	2.6943
Standard Error	0.0209
Median	2.6778
Mode	#N/A
Standard Deviation	0.0512
Sample Variance	0.0026
Kurtosis	-1.5459
Skewness	0.5967
Range	0.1274
Largest(1)	2.7637
Smallest(1)	2.6363
Confidence Level(95.0%)	0.0537

APPENDIX B: XRF ELEMENTAL COMPOSITION OF THE BULK SEDIMENT

XRF FOR LAURA TAYLOR JULY 14, 2005
CALIBRATION USED: CALSOILS_090204

GSD-11 is a standard

Sample	Sum of conc. (%)	Al2O3 Al (%)	CaO Ca (%)	Fe2O3 Fe (%)	K2O K (%)	MgO Mg (%)	MnO Mn (%)	Na2O Na (%)	P2O5 P (%)	SiO2 Si (%)	TiO2 Ti (%)
GSD-11	96.443	10.350	0.446	4.214	3.153	0.589	0.305	0.486	0.064	76.217	0.356
DEPTH (cm)											
0-3	88.605	16.240	0.922	6.263	3.477	3.133	0.083	2.657	0.178	54.599	0.741
3-5	89.542	16.465	0.893	6.341	3.546	3.112	0.070	2.705	0.168	55.171	0.755
5-7	89.976	16.649	0.840	6.532	3.588	3.060	0.071	2.410	0.160	55.556	0.766
7-9	90.309	16.695	0.850	6.584	3.609	3.042	0.072	2.331	0.157	55.775	0.771
9-11	90.188	16.614	0.852	6.653	3.604	3.026	0.072	2.360	0.154	55.623	0.768
11-16	90.381	16.694	0.868	6.637	3.644	3.052	0.074	2.273	0.153	55.724	0.780

XRF FOR LAURA TAYLOR JULY 14, 2005
CALIBRATION USED: CALSOILS_090204

GSD-11 is a standard

Sample	As As (ppm)	Ba Ba (ppm)	Co Co (ppm)	Cr Cr (ppm)	Cu Cu (ppm)	Hf Hf (ppm)	Nb Nb (ppm)	Ni Ni (ppm)	Pb Pb (ppm)	Rb Rb (ppm)	S S (ppm)	Sr Sr (ppm)	V V (ppm)	W W (ppm)	Y Y (ppm)	Zn Zn (ppm)	Zr Zr (ppm)
GSD-11	108	249	14	45	75	5	26	16	780	405	188	31	35	106	38	366	148
DEPTH (cm)																	
0-3	18	435	8	96	22	4	13	44	19	154	1875	116	85	-40	27	113	131
3-5	17	456	9	96	22	6	13	45	19	157	1876	115	87	-41	28	115	134
5-7	18	459	10	98	23	6	13	46	20	157	2151	114	90	-42	29	115	138
7-9	18	440	10	98	22	5	14	45	25	157	2955	114	91	-42	28	112	142
9-11	18	451	10	97	22	6	14	46	23	156	3339	114	86	-41	29	112	142
11-16	18	454	10	98	21	2	13	46	21	156	3536	114	89	-41	29	111	139

Minus sign indicated measured value is below the background noise

APPENDIX C: XRD MINERALOGICAL COMPOSITION

Silt-Size Particle Fraction

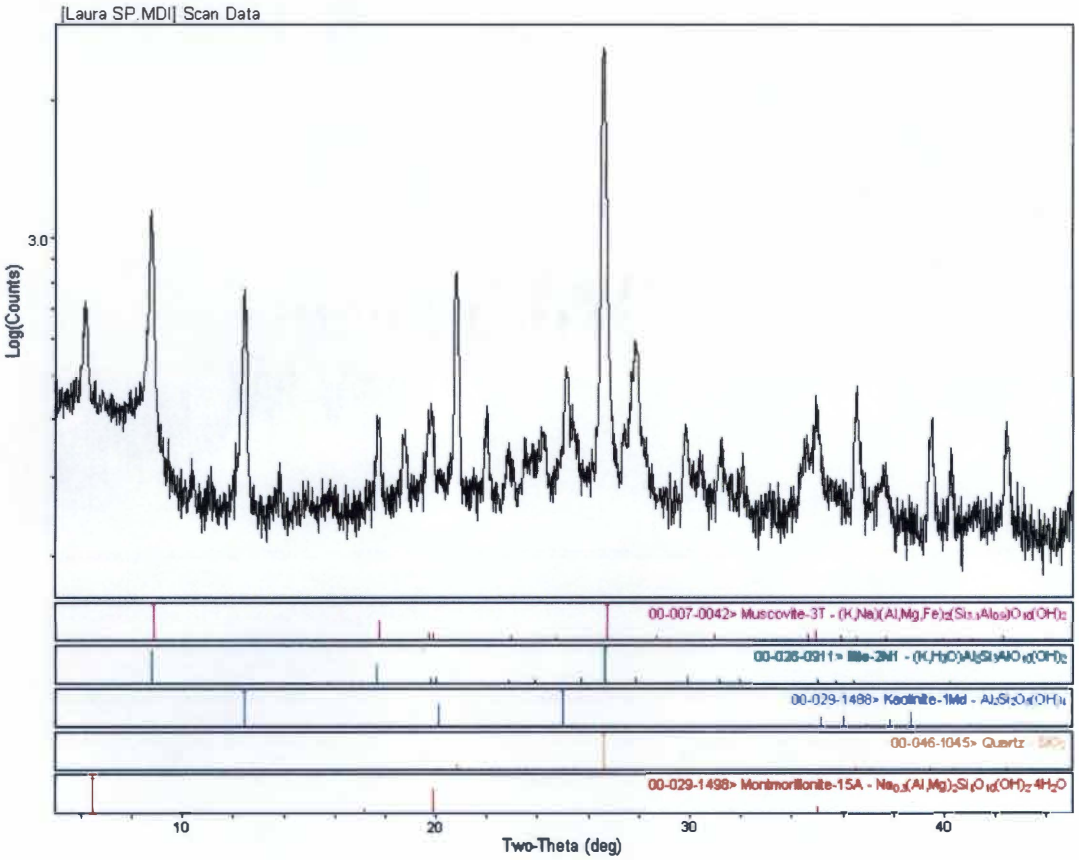

Silt-Size Aggregate Fraction

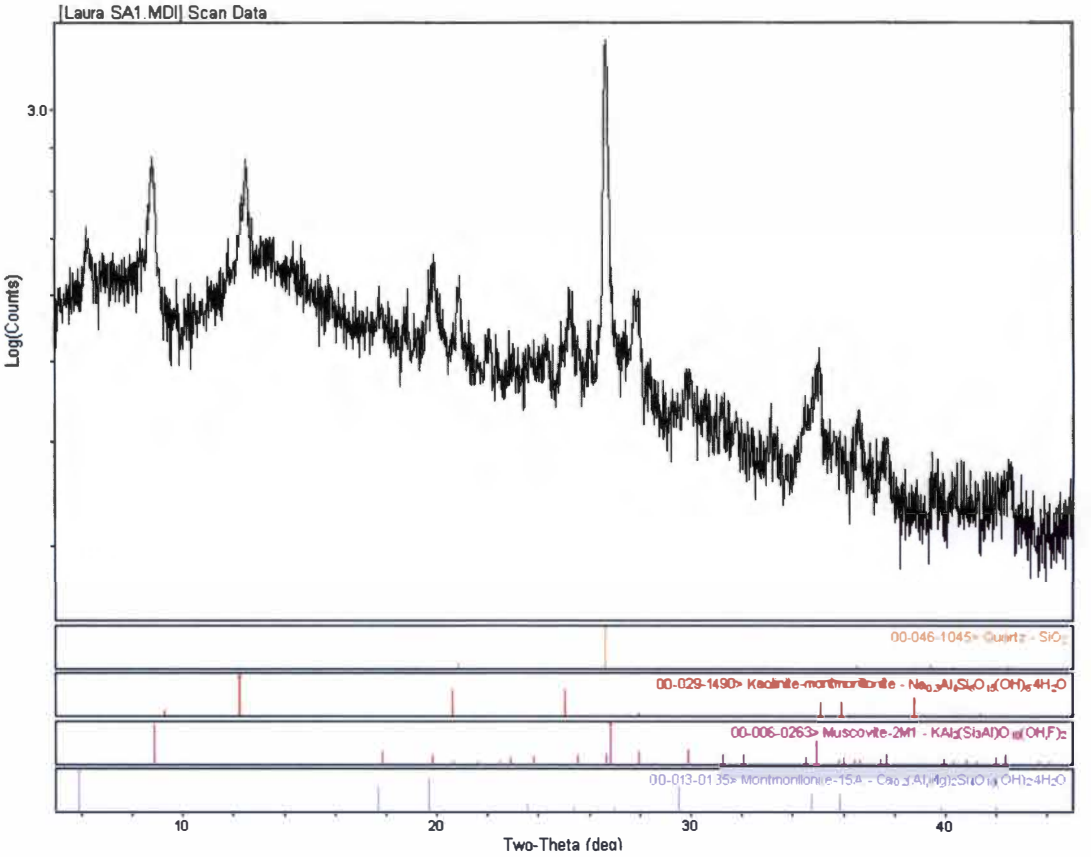

Clay-Size Particle Fraction

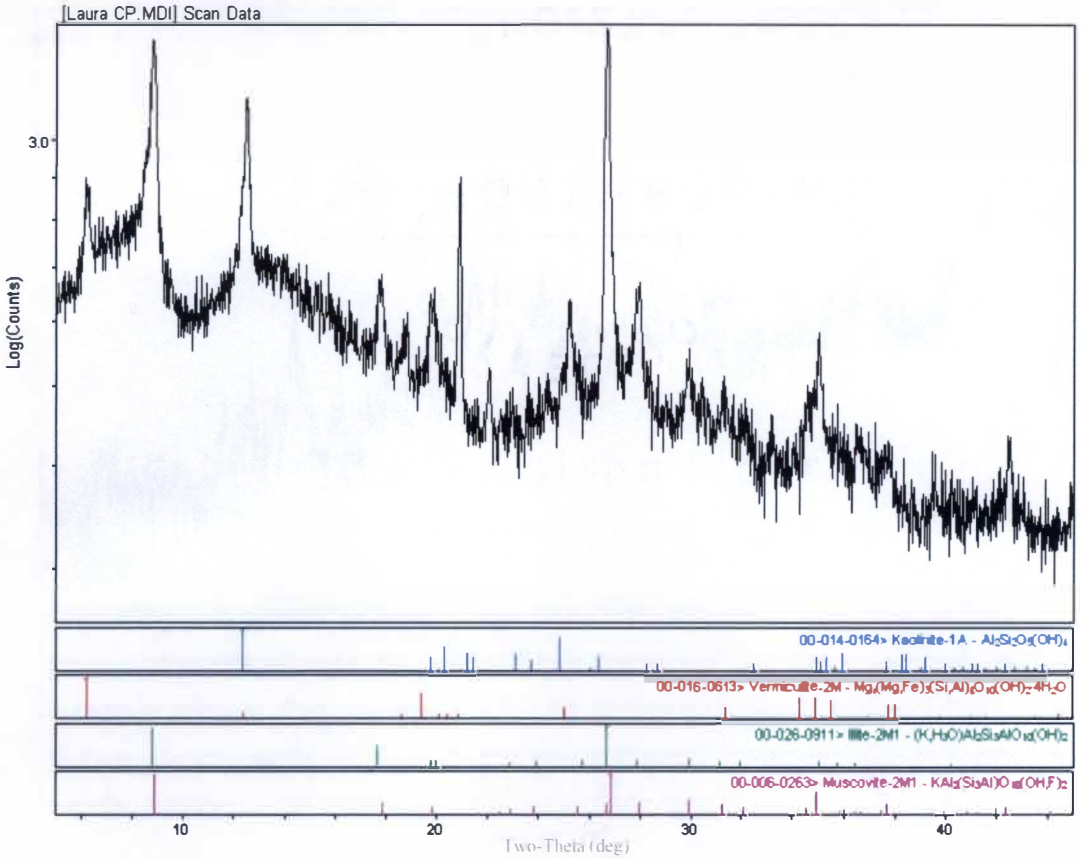

Clay-Size Aggregate Fraction

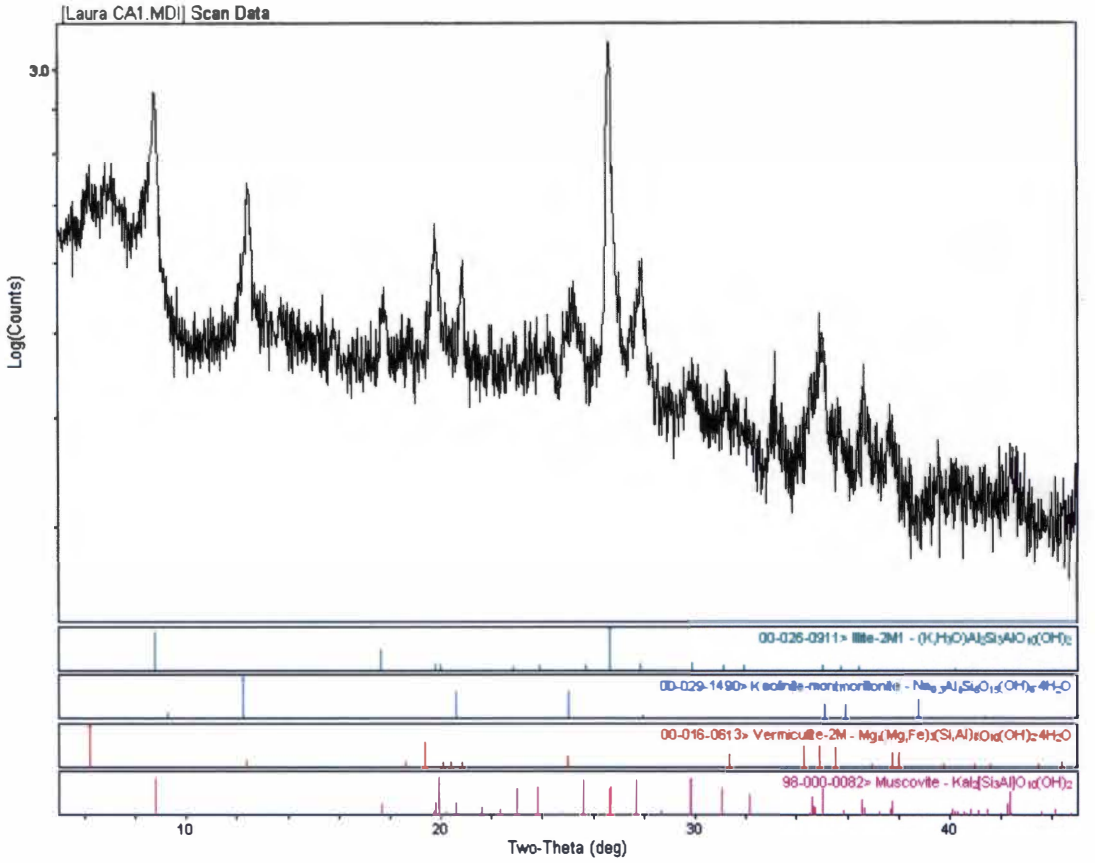

APPENDIX D: FLOW CYTOMETER DATA

Silt-Size Aggregate Dot Plots

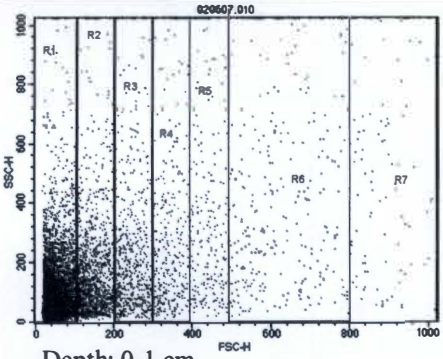

Depth: 0-1 cm

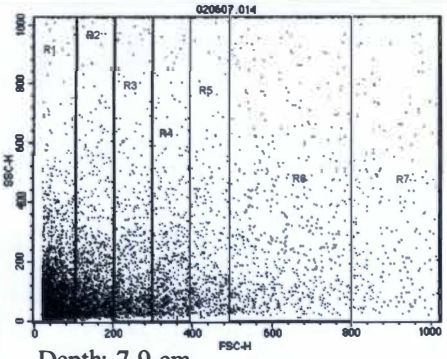

Depth: 7-9 cm

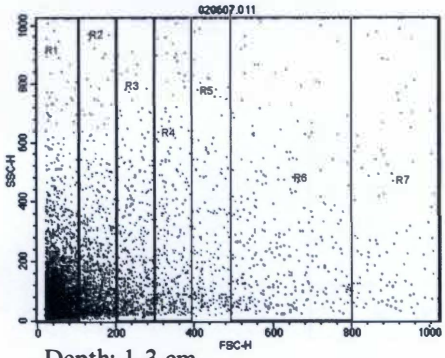

Depth: 1-3 cm

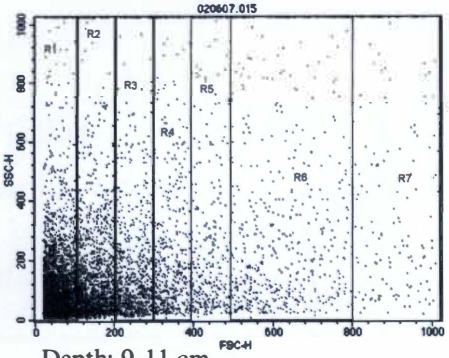

Depth: 9-11 cm

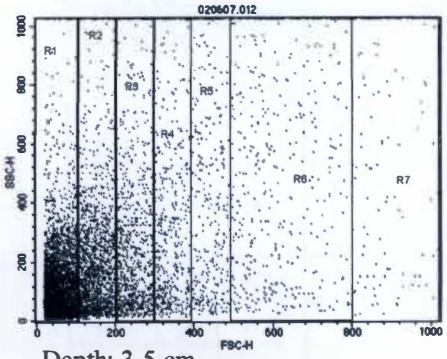

Depth: 3-5 cm

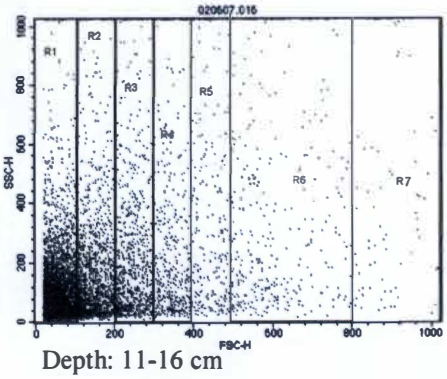

Depth: 11-16 cm

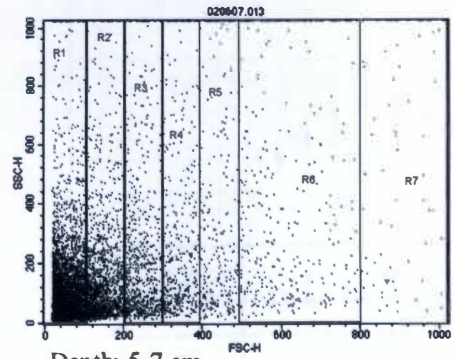

Depth: 5-7 cm

Silt-Size Aggregate Data

	Marker	Events	% Total	Mean	CV	Median	Peak
Silt: 0-1 cm	All	10000	100.0	123.4	141.2	52.0	23
	M1	7009	70.1	44.2	46.5	38.0	23
	M2	1399	14.0	136.2	20.7	132.0	109
	M3	657	6.6	243.1	12.7	241.0	199
	M4	341	3.4	348.7	8.1	349.0	313
	M5	222	2.2	450.5	6.4	450.0	484
	M6	317	3.2	628.9	13.7	614.0	501
	M7	112	1.1	875.6	6.7	872.0	799
Silt: 1-3 cm	All	10000	100.0	123.6	142.1	51.0	23
	M1	7024	70.2	43.3	46.0	37.0	23
	M2	1351	13.5	137.8	20.4	134.0	110
	M3	622	6.2	243.6	12.5	240.0	236
	M4	365	3.7	349.2	8.2	347.0	375
	M5	216	2.2	448.9	6.6	447.0	404
	M6	340	3.4	623.1	13.7	610.0	581
	M7	108	1.1	882.1	6.4	880.5	814
Silt: 3-5 cm	All	10000	100.0	152.0	126.2	68.0	23
	M1	6074	60.7	45.7	46.8	39.0	23
	M2	4659	46.6	139.9	20.5	136.0	110
	M3	899	9.0	243.2	12.6	241.0	214
	M4	503	5.0	347.5	8.5	345.0	323
	M5	328	3.3	447.9	6.3	447.0	414
	M6	457	4.6	625.7	13.4	612.0	516
	M7	128	1.3	882.4	6.6	871.0	876
Silt: 5-7 cm	All	10000	100.0	128.8	129.2	60.0	23
	M1	6572	65.7	45.7	46.8	39.0	23
	M2	1629	16.3	137.7	20.5	134.0	105
	M3	796	8.0	241.1	12.4	237.0	214
	M4	410	4.1	348.1	8.3	346.0	307
	M5	260	2.6	450.2	6.4	451.0	419
	M6	330	3.3	615.3	13.7	599.0	500
	M7	70	0.7	886.6	6.5	881.0	922

	Marker	Events	% Total	Mean	CV	Median	Peak
Silt: 7-9 cm	All	10000	100.0	197.4	121.4	85.0	23
	M1	5350	53.5	44.9	46.4	39.0	23
	M2	1601	16.0	140.7	20.5	138.0	97
	M3	961	9.6	243.3	12.9	242.0	195
	M4	650	6.5	350.1	8.3	347.0	325
	M5	398	4.0	448.4	6.4	447.0	403
	M6	733	7.3	628.9	13.6	618.0	542
	M7	254	2.5	885.1	6.9	875.5	818
Silt: 9-11 cm	All	10000	100.0	161.0	128.7	70.0	23
	M1	5951	59.5	45.7	46.3	40.0	23
	M2	1700	17.0	140.0	20.9	137.0	102
	M3	889	8.9	242.9	13.0	240.0	208
	M4	499	5.0	347.6	8.3	345.0	307
	M5	301	3.0	449.6	6.3	448.0	448
	M6	505	5.1	626.7	13.5	617.0	507
	M7	151	1.5	893.2	6.7	886.0	949
Silt: 11-16 cm	All	10000	100.0	131.2	125.6	63.0	23
	M1	6408	64.1	46.0	45.9	40.0	23
	M2	1697	17.0	137.7	20.7	133.0	113
	M3	889	8.9	241.3	12.4	239.0	218
	M4	443	4.4	348.7	8.0	345.0	342
	M5	249	2.5	452.2	6.7	454.0	463
	M6	327	3.3	610.3	13.8	590.0	543
	M7	74	0.7	880.3	6.0	872.5	797

Clay-Size Aggregate Dot Plots

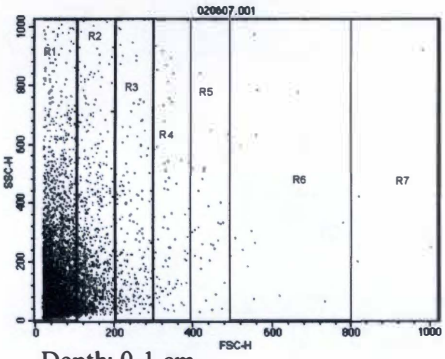

Depth: 0-1 cm

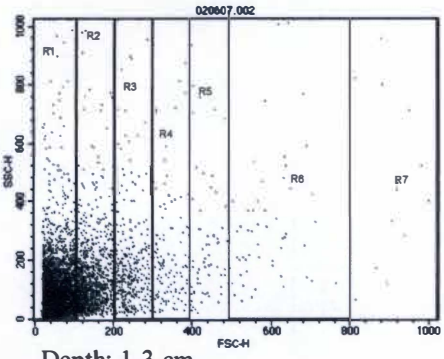

Depth: 1-3 cm

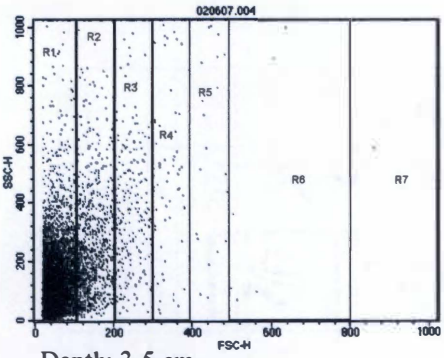

Depth: 3-5 cm

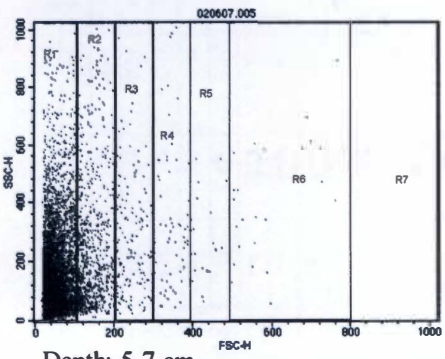

Depth: 5-7 cm

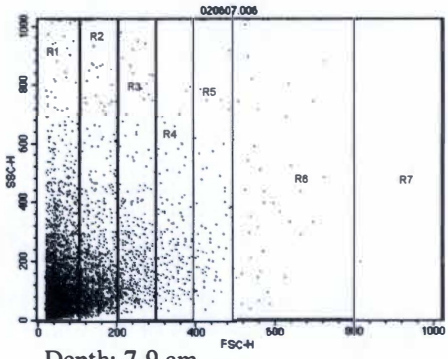

Depth: 7-9 cm

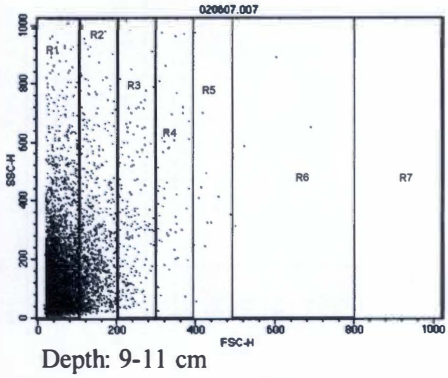

Depth: 9-11 cm

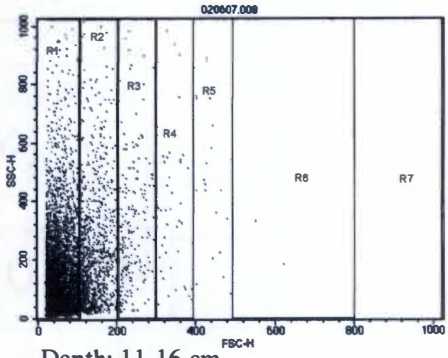

Depth: 11-16 cm

Clay Aggregate Data

	Marker	Events	% Total	Mean	CV	Median	Peak
Clay: 0-1 cm	All	10000	100.00	65.68	102.09	43.0	23
	M1	8400	84.00	44.01	46.32	38.0	23
	M2	1314	13.14	130.82	20.30	125.0	104
	M3	279	2.79	235.58	12.78	229.0	203
	M4	82	0.82	342.94	8.15	337.0	335
	M5	37	0.37	446.62	6.15	447.0	403
	M6	22	0.22	591.95	14.32	558.0	506
	M7	5	0.05	870.60	7.91	845.0	818
Clay: 1-3 cm	All	10000	100.00	72.08	113.97	43.0	23
	M1	8127	81.27	43.18	46.25	37.0	23
	M2	1383	13.83	134.47	21.34	128.0	103
	M3	392	3.92	235.61	14.56	231.5	194
	M4	121	1.21	348.79	8.20	346.0	305
	M5	62	0.62	443.47	6.44	441.0	413
	M6	42	0.42	614.50	13.51	607.5	502
	M7	8	0.08	885.62	7.50	873.5	802
Clay: 3-5 cm	All	10000	100.00	62.91	102.19	40.0	23
	M1	8521	85.21	42.29	46.08	36.0	23
	M2	1152	11.52	133.99	20.74	128.0	100
	M3	331	3.31	236.20	13.18	231.0	197
	M4	68	0.68	342.71	7.97	340.0	318
	M5	29	0.29	448.45	6.10	441.0	427
	M6	13	0.13	603.00	12.87	584.0	505
	M7	5	0.05	877.40	7.00	860.0	813
Clay: 5-7 cm	All	10000	100.00	59.05	103.64	39.0	23
	M1	8764	87.64	41.59	45.89	36.0	23
	M2	976	9.76	132.42	20.68	125.0	103
	M3	230	2.30	237.50	13.53	232.0	194
	M4	74	0.74	353.45	8.04	348.0	316
	M5	24	0.24	442.42	6.86	438.0	405
	M6	26	0.26	599.19	15.47	571.0	503
	M7	1	0.01	895.00	***	895.0	894

	Marker	Events	% Total	Mean	CV	Median	Peak
Clay: 7-9 cm	All	10000	100.00	78.12	102.92	48.0	23
	M1	7834	78.34	45.70	45.49	40.0	23
	M2	1550	15.50	134.47	21.18	128.0	104
	M3	493	4.93	236.96	12.87	234.0	202
	M4	167	1.67	347.35	8.49	349.0	303
	M5	71	0.71	441.85	6.38	436.0	423
	M6	45	0.45	586.53	10.66	569.0	516
	M7	2	0.02	812.00	0.70	812.0	808
Clay: 9-11 cm	All	10000	100.00	61.62	86.51	43.0	23
	M1	8544	85.44	44.28	45.37	38.0	23
	M2	1251	12.51	131.89	20.35	126.0	108
	M3	246	2.46	233.35	11.98	229.0	194
	M4	58	0.58	340.24	8.25	335.0	306
	M5	10	0.10	437.60	6.31	426.5	408
	M6	6	0.06	572.50	13.14	562.5	502
	M7	1	0.01	904.00	***	904.0	904
Clay: 11-16 cm	All	10000	100.00	62.35	104.48	40.0	23
	M1	8613	86.13	42.27	45.76	36.0	23
	M2	1074	10.74	132.18	20.31	126.0	99
	M3	275	2.75	238.93	12.79	237.0	215
	M4	89	0.89	347.35	8.30	344.0	311
	M5	38	0.38	443.66	6.61	438.0	435
	M6	25	0.25	560.68	8.52	547.0	516
	M7	3	0.03	921.67	4.02	934.0	880

Sonicated Silt-Size Aggregate Dot Plots

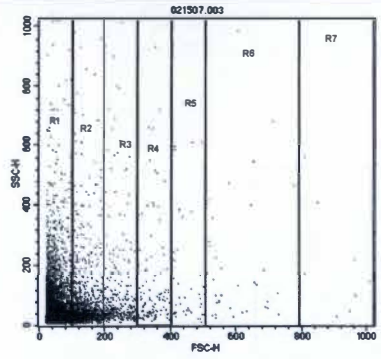

Depth 0-1 cm (2000 J)

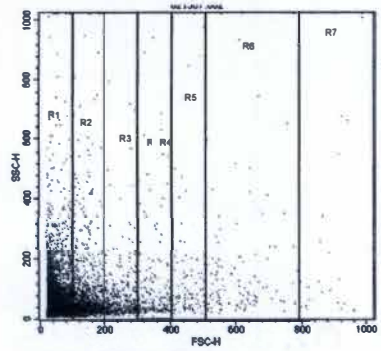

Depth 1-3 cm (2000 J)

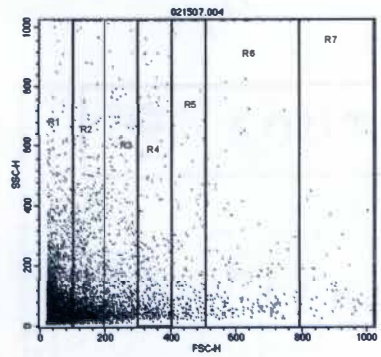

Depth 3-5 cm (2000 J)

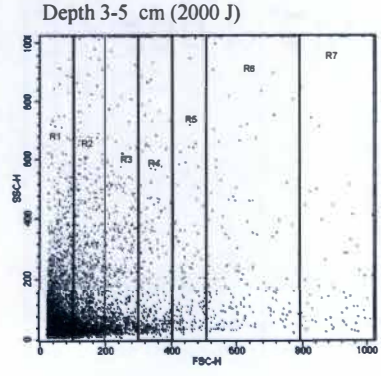

Depth 5-7 cm (1000 J)

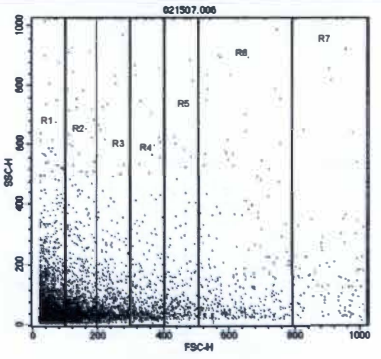

Depth 7-9 cm (2000 J)

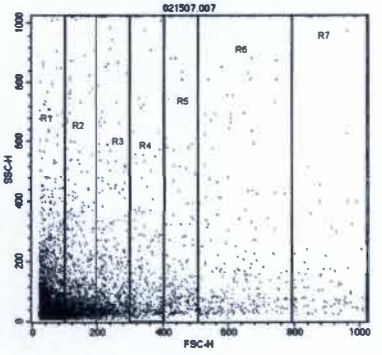

Depth 9-11 cm (2000 J)

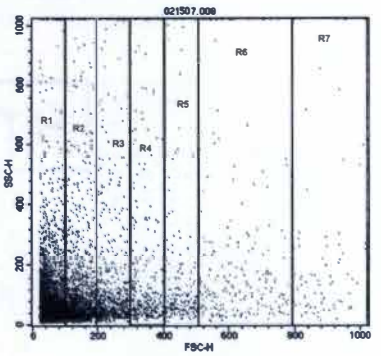

Depth 11-16 cm (600 J)

Sonicated Silt-Size Aggregate Data

	Marker	Events	% Total	Mean	CV	Median	Peak
Silt: 0-1 cm (2000 J/mL)	All	10000	100.0	81.3	136.0	43.0	24
	M1	8062	80.6	43.1	46.3	37.0	24
	M2	1172	11.7	138.7	20.1	135.0	101
	M3	351	3.5	246.3	11.7	244.0	207
	M4	183	1.8	346.0	8.8	343.0	302
	M5	89	0.9	448.7	6.4	445.0	444
	M6	118	1.2	607.1	13.3	600.0	541
	M7	23	0.2	895.0	6.0	902.0	922
Silt: 1-3 cm (2000 J/mL)	All	10000	100.0	67.8	119.4	41.0	24
	M1	8410	84.1	42.3	45.9	36.0	24
	M2	1104	11.0	137.7	20.8	132.0	114
	M3	288	2.9	242.3	11.6	237.0	219
	M4	121	1.2	345.1	8.0	342.0	328
	M5	42	0.4	449.9	7.1	448.0	413
	M6	43	0.4	596.1	12.9	580.0	506
	M7	9	0.1	898.0	8.6	907.0	810
Silt: 3-5 cm (2000 J/mL)	All	10000	100.0	106.1	136.3	50.0	24
	M1	7211	72.1	43.9	46.0	38.0	24
	M2	1478	14.8	141.2	20.2	138.0	100
	M3	562	5.6	243.5	11.4	242.0	207
	M4	317	3.2	343.6	8.3	342.0	301
	M5	166	1.7	447.7	6.7	446.0	407
	M6	204	2.0	615.8	13.2	597.0	565
	M7	42	0.4	901.9	6.5	900.0	839
Silt: 5-7 cm (1000 J/mL)	All	10000	100.0	108.9	139.0	51.0	24
	M1	7184	71.8	44.8	46.3	38.0	24
	M2	1519	15.2	141.9	20.7	139.0	100
	M3	535	5.4	244.3	11.2	242.0	204
	M4	314	3.1	34388.0	8.1	340.0	328
	M5	159	1.6	447.1	6.4	440.0	433
	M6	195	2.0	618.5	14.5	600.0	514
	M7	67	0.7	910.6	6.9	925.0	812

	Marker	Events	% Total	Mean	CV	Median	Peak
Silt: 7-9 cm (2000 J/mL)	All	10000	100.0	131.2	142.2	54.0	24
	M1	6812	68.1	44.4	46.6	39.0	24
	M2	1480	14.8	141.9	20.6	136.0	108
	M3	573	5.7	244.4	11.4	242.0	210
	M4	360	3.6	345.1	8.5	343.0	306
	M5	232	2.3	446.0	6.3	444.0	439
	M6	349	3.5	623.8	13.4	617.0	520
	M7	107	1.1	914.9	7.3	889.0	821
Silt: 9-11 cm (2000 J/mL)	All	10000	100.0	119.1	144.7	51.0	24
	M1	7169	71.7	44.4	45.8	38.0	24
	M2	1298	13.0	141.9	20.1	138.0	110
	M3	568	5.7	243.0	11.6	238.0	204
	M4	299	3.0	344.8	8.7	341.0	308
	M5	209	2.1	447.8	6.4	445.0	456
	M6	292	2.9	626.6	13.3	613.0	527
	M7	92	0.9	895.6	7.0	894.0	840
Silt: 11-16 cm (600 J/mL)	All	10000	100.0	115.8	141.1	63.0	23
	M1	7048	70.5	45.5	46.2	40.0	23
	M2	1550	15.5	141.0	20.8	133.0	113
	M3	572	5.7	243.4	11.7	239.0	218
	M4	394	3.9	342.5	8.3	345.0	342
	M5	188	1.9	447.2	6.6	454.0	463
	M6	222	2.2	628.4	13.5	590.0	543
	M7	72	0.7	895.5	6.8	872.5	797

APPENDIX E: XDC SIZE DATA

Silt-Size Aggregate

0-1cm					
% Less Than	size (um)	Differential	% Less Than	size (um)	Differential
9.00	0.784	500.00	54.00	0.93	250.00
10.00	0.786	333.33	55.00	0.94	333.33
11.00	0.789	500.00	56.00	0.94	200.00
12.00	0.791	333.33	57.00	0.95	142.86
13.00	0.794	500.00	58.00	0.95	166.67
14.00	0.796	333.33	59.00	0.96	142.86
15.00	0.799	333.33	60.00	0.97	142.86
16.00	0.802	333.33	61.00	0.97	125.00
17.00	0.805	250.00	62.00	0.98	111.11
18.00	0.809	333.33	63.00	0.99	125.00
19.00	0.812	250.00	64.00	1.00	47.62
20.00	0.816	250.00	65.00	1.02	50.00
21.00	0.820	333.33	66.00	1.04	52.63
22.00	0.823	250.00	67.00	1.06	21.74
23.00	0.827	500.00	68.00	1.10	2.22
24.00	0.829	500.00	69.00	1.55	11.49
25.00	0.831	333.33	70.00	1.64	2.00
26.00	0.834	500.00	71.00	2.14	9.90
27.00	0.836	500.00	72.00	2.24	9.35
28.00	0.838	333.33	73.00	2.35	14.49
29.00	0.841	500.00	74.00	2.42	16.95
30.00	0.843	500.00	75.00	2.48	16.13
31.00	0.845	250.00	76.00	2.54	15.15
32.00	0.849	333.33	77.00	2.60	7.25
33.00	0.852	250.00	78.00	2.74	2.58
34.00	0.856	250.00	79.00	3.13	2.32
35.00	0.860	333.33	80.00	3.56	4.65
36.00	0.863	250.00	81.00	3.78	3.80
37.00	0.867	250.00	82.00	4.04	0.51
38.00	0.871	333.33	83.00	5.98	2.28
39.00	0.874	250.00	84.00	6.42	2.61
40.00	0.878	250.00	85.00	6.80	4.48
41.00	0.882	250.00	86.00	7.03	4.02
42.00	0.886	250.00	87.00	7.28	3.68
43.00	0.890	250.00	88.00	7.55	3.79
44.00	0.894	250.00	89.00	7.81	3.80
45.00	0.898	200.00	90.00	8.07	3.65
46.00	0.903	250.00	91.00	8.35	3.65
47.00	0.907	250.00	92.00	8.62	3.39
48.00	0.911	250.00	93.00	8.92	3.24
49.00	0.915	250.00	94.00	9.23	3.25
50.00	0.919	250.00	95.00	9.53	2.33
51.00	0.923	250.00	96.00	9.96	2.25
52.00	0.927	250.00	97.00	10.41	1.87
53.00	0.931	333.33	98.00	10.94	1.41
			99.00	11.65	8.50

1-3 cm		
% Less Than	size (um)	Differential
71	0.536	21.74
72	0.582	17.54
73	0.639	4.03
74	0.887	0.84
75	2.080	3.44
76	2.371	5.59
77	2.550	5.35
78	2.737	6.54
79	2.890	5.78
80	3.063	9.17
81	3.172	10.87
82	3.264	10.64
83	3.358	12.50
84	3.438	14.49
85	3.507	15.38
86	3.572	10.99
87	3.663	10.00
88	3.763	11.24
89	3.852	9.80
90	3.954	8.62
91	4.070	8.55
92	4.187	7.35
93	4.323	3.70
94	4.593	5.71
95	4.768	3.65
96	5.042	2.91
97	5.386	2.51
98	5.785	2.35
99	6.210	

Silt-Size Aggregate (continued)

3-5 cm					
% Less Than	size (um)	Differential	% Less Than	size (um)	Differential
36.00	0.536	21.74	67.00	4.027	14.29
37.00	0.582	20.41	68.00	4.097	11.11
38.00	0.631	8.06	69.00	4.187	10.00
39.00	0.755	18.52	70.00	4.287	12.35
40.00	0.809	500.00	71.00	4.368	4.98
41.00	0.811	333.33	72.00	4.569	15.63
42.00	0.814	500.00	73.00	4.633	12.20
43.00	0.816	500.00	74.00	4.715	8.77
44.00	0.818	333.33	75.00	4.829	9.26
45.00	0.821	37.04	76.00	4.937	12.20
46.00	0.848	9.35	77.00	5.019	7.81
47.00	0.955	1.42	78.00	5.147	5.78
48.00	1.660	3.72	79.00	5.320	5.95
49.00	1.929	5.95	80.00	5.488	4.88
50.00	2.097	5.75	81.00	5.693	4.26
51.00	2.271	8.33	82.00	5.928	3.75
52.00	2.391	7.30	83.00	6.195	5.43
53.00	2.528	7.63	84.00	6.379	3.27
54.00	2.659	6.99	85.00	6.685	3.50
55.00	2.802	5.46	86.00	6.971	4.12
56.00	2.985	9.52	87.00	7.214	4.63
57.00	3.090	9.09	88.00	7.430	4.72
58.00	3.200	9.80	89.00	7.642	4.90
59.00	3.302	8.33	90.00	7.846	4.90
60.00	3.422	12.35	91.00	8.050	3.95
61.00	3.503	12.66	92.00	8.303	3.77
62.00	3.582	16.39	93.00	8.568	3.69
63.00	3.643	11.76	94.00	8.839	3.55
64.00	3.728	8.93	95.00	9.121	3.55
65.00	3.840	9.62	96.00	9.403	3.30
66.00	3.944	12.05	97.00	9.706	3.01
			98.00	10.038	3.02
			99.00	10.369	9.55

7-9 cm					
% Less Than	size (um)	Differential	% Less Than	size (um)	Differential
9	0.704	500.00	54	0.854	250.00
10	0.706	333.33	55	0.858	333.33
11	0.709	500.00	56	0.861	200.00
12	0.711	333.33	57	0.866	142.86
13	0.714	500.00	58	0.873	166.67
14	0.716	333.33	59	0.879	142.86
15	0.719	333.33	60	0.886	142.86
16	0.722	333.33	61	0.893	125.00
17	0.725	250.00	62	0.901	111.11
18	0.729	333.33	63	0.910	125.00
19	0.732	250.00	64	0.918	47.62
20	0.736	250.00	65	0.939	50.00
21	0.740	333.33	66	0.959	166.67
22	0.743	250.00	67	0.965	66.67
23	0.747	500.00	68	0.980	66.67
24	0.749	500.00	69	0.995	4.39
25	0.751	333.33	70	1.223	11.11
26	0.754	500.00	71	1.313	22.22
27	0.756	500.00	72	1.358	43.48
28	0.758	333.33	73	1.381	45.45
29	0.761	500.00	74	1.403	43.48
30	0.763	500.00	75	1.426	45.45
31	0.765	250.00	76	1.448	58.82
32	0.769	333.33	77	1.465	58.82
33	0.772	250.00	78	1.482	66.67
34	0.776	250.00	79	1.497	66.67
35	0.780	333.33	80	1.512	66.67
36	0.783	250.00	81	1.527	90.91
37	0.787	250.00	82	1.538	83.33
38	0.791	333.33	83	1.550	83.33
39	0.794	250.00	84	1.562	83.33
40	0.798	250.00	85	1.574	83.33
41	0.802	250.00	86	1.586	83.33
42	0.806	250.00	87	1.598	71.43
43	0.810	250.00	88	1.612	58.82
44	0.814	250.00	89	1.629	58.82
45	0.818	200.00	90	1.646	58.82
46	0.823	250.00	91	1.663	58.82
47	0.827	250.00	92	1.680	62.50
48	0.831	250.00	93	1.696	58.82
49	0.835	250.00	94	1.713	76.92
50	0.839	250.00	95	1.726	76.92
51	0.843	250.00	96	1.739	41.67
52	0.847	250.00	97	1.763	33.33
53	0.851	333.33	98	1.793	33.33
			99	1.823	

Silt-Size Aggregate (continued)

9-11 cm		
% Less Than	size (um)	Differential
84	0.604	7.25
85	0.742	2.54
86	1.136	7.52
87	1.269	5.85
88	1.44	5.13
89	1.635	5.99
90	1.802	6.33
91	1.96	2.59
92	2.346	4.95
93	2.548	7.25
94	2.686	7.52
95	2.819	5.24
96	3.01	3.48
97	3.297	0.73
98	4.663	0.56
99	6.463	15.32

11-16cm		
% Less Than	size (um)	Differential
85	0.531	1.85
86	1.073	8.20
87	1.195	5.65
88	1.372	2.44
89	1.781	2.49
90	2.183	5.85
91	2.354	5.10
92	2.55	3.77
93	2.815	2.04
94	3.304	1.26
95	4.099	0.24
96	8.31	1.04
97	9.275	0.91
98	10.372	0.71
99	11.771	8.41

Clay-Size Aggregate

0-1cm					
% Less Than	size (um)	Differential	% Less Than	size (um)	Differential
8.00	0.022	166.67	50.00	0.330	250.00
9.00	0.028	166.67	51.00	0.334	250.00
10.00	0.034	83.33	52.00	0.338	200.00
11.00	0.046	111.11	53.00	0.343	250.00
12.00	0.055	250.00	54.00	0.347	250.00
13.00	0.059	250.00	55.00	0.351	250.00
14.00	0.063	71.43	56.00	0.355	250.00
15.00	0.077	333.33	57.00	0.359	200.00
16.00	0.080	200.00	58.00	0.364	250.00
17.00	0.085	250.00	59.00	0.368	250.00
18.00	0.089	500.00	60.00	0.372	250.00
19.00	0.091	1000.00	61.00	0.376	250.00
20.00	0.092	1000.00	62.00	0.380	333.33
21.00	0.093	1000.00	63.00	0.383	250.00
22.00	0.094	1000.00	64.00	0.387	250.00
23.00	0.095	#DIV/0!	65.00	0.391	250.00
24.00	0.095	1000.00	66.00	0.395	250.00
25.00	0.096	#DIV/0!	67.00	0.399	166.67
26.00	0.096	1000.00	68.00	0.405	200.00
27.00	0.097	#DIV/0!	69.00	0.410	166.67
28.00	0.097	1000.00	70.00	0.416	200.00
29.00	0.098	#DIV/0!	71.00	0.421	250.00
30.00	0.098	1000.00	72.00	0.425	200.00
31.00	0.099	#DIV/0!	73.00	0.430	111.11
32.00	0.099	500.00	74.00	0.439	111.11
33.00	0.101	111.11	75.00	0.448	125.00
34.00	0.110	16.67	76.00	0.456	142.86
35.00	0.170	33.33	77.00	0.463	66.67
36.00	0.200	28.57	78.00	0.478	62.50
37.00	0.235	58.82	79.00	0.494	55.56
38.00	0.252	66.67	80.00	0.512	7.87
39.00	0.267	125.00	81.00	0.639	9.71
40.00	0.275	142.86	82.00	0.742	14.71
41.00	0.282	142.86	83.00	0.810	23.26
42.00	0.289	166.67	84.00	0.853	17.54
43.00	0.295	125.00	85.00	0.910	23.26
44.00	0.303	166.67	86.00	0.953	19.61
45.00	0.309	250.00	87.00	1.004	23.81
46.00	0.313	250.00	88.00	1.046	24.39
47.00	0.317	250.00	89.00	1.087	21.74
48.00	0.321	200.00	90.00	1.133	24.39
49.00	0.326	250.00	91.00	1.174	25.00
			92.00	1.214	19.23
			93.00	1.266	19.23
			94.00	1.318	18.87
			95.00	1.371	18.87
			96.00	1.424	14.71
			97.00	1.492	12.99
			98.00	1.569	8.40
			99.00	1.688	58.65

1-3 cm		
% Less Than	size (um)	Differential
90.00	0.189	11.90
91.00	0.273	18.18
92.00	0.328	19.61
93.00	0.379	3.80
94.00	0.642	11.36
95.00	0.730	10.64
96.00	0.824	9.09
97.00	0.934	3.79
98.00	1.198	3.91
99.00	1.454	

Clay-Size Aggregate (continued)

3-5 cm					
% Less Than	size (um)	Differential	% Less Than	size (um)	Differential
32.00	0.090	90.91	66.00	1.90	38.46
33.00	0.101	125.00	67.00	1.92	5.68
34.00	0.109	71.43	68.00	2.10	5.00
35.00	0.123	37.04	69.00	2.30	5.00
36.00	0.150	100.00	70.00	2.50	3.33
37.00	0.160	45.45	71.00	2.80	20.00
38.00	0.182	66.67	72.00	2.85	20.00
39.00	0.197	125.00	73.00	2.90	5.00
40.00	0.205	142.86	74.00	3.10	20.00
41.00	0.212	142.86	75.00	3.15	25.00
42.00	0.219	166.67	76.00	3.19	16.67
43.00	0.225	125.00	77.00	3.25	9.09
44.00	0.233	166.67	78.00	3.36	33.33
45.00	0.239	250.00	79.00	3.39	5.88
46.00	0.243	250.00	80.00	3.56	9.09
47.00	0.247	250.00	81.00	3.67	50.00
48.00	0.251	200.00	82.00	3.69	6.67
49.00	0.256	250.00	83.00	3.84	12.50
50.00	0.260	250.00	84.00	3.92	7.14
51.00	0.264	250.00	85.00	4.06	7.14
52.00	0.268	200.00	86.00	4.20	3.33
53.00	0.273	250.00	87.00	4.50	10.00
54.00	0.277	250.00	88.00	4.60	11.11
55.00	0.281	250.00	89.00	4.69	7.14
56.00	0.285	250.00	90.00	4.83	11.11
57.00	0.289	200.00	91.00	4.92	5.88
58.00	0.294	250.00	92.00	5.09	5.00
59.00	0.298	250.00	93.00	5.29	2.33
60.00	0.302	250.00	94.00	5.72	9.09
61.00	1.20	1.68	95.00	5.83	3.33
62.00	1.79	58.82	96.00	6.13	2.70
63.00	1.81	58.82	97.00	6.50	3.33
64.00	1.83	34.48	98.00	6.80	1.43
65.00	1.86	24.39	99.00	7.50	

5-7 cm		
% Less Than	size (um)	Differential
84.00	0.04	30.30
85.00	0.07	125.00
86.00	0.08	111.11
87.00	0.09	90.91
88.00	0.10	41.67
89.00	0.12	9.43
90.00	0.23	14.08
91.00	0.30	12.99
92.00	0.38	27.03
93.00	0.41	23.81
94.00	0.46	17.86
95.00	0.51	9.26
96.00	0.62	8.62
97.00	0.74	9.43
98.00	0.84	10.99
99.00	0.93	106.11

Clay-size Aggregate (continued)

7-9 cm					
% Less Than	size (um)	Differential	% Less Than	size (um)	Differential
23.00	0.020	500.00	61.00	0.314	166.67
24.00	0.022	166.67	62.00	0.320	166.67
25.00	0.028	83.33	63.00	0.326	166.67
26.00	0.040	111.11	64.00	0.332	142.86
27.00	0.049	250.00	65.00	0.339	166.67
28.00	0.053	250.00	66.00	0.345	142.86
29.00	0.057	71.43	67.00	0.352	166.67
30.00	0.071	333.33	68.00	0.358	142.86
31.00	0.074	200.00	69.00	0.365	125.00
32.00	0.079	250.00	70.00	0.373	166.67
33.00	0.083	500.00	71.00	0.379	142.86
34.00	0.085	1000.00	72.00	0.386	166.67
35.00	0.086	1000.00	73.00	0.392	166.67
36.00	0.087	1000.00	74.00	0.398	125.00
37.00	0.088	1000.00	75.00	0.406	111.11
38.00	0.089	#DIV/0!	76.00	0.415	111.11
39.00	0.089	1000.00	77.00	0.424	90.91
40.00	0.090	#DIV/0!	78.00	0.435	90.91
41.00	0.090	1000.00	79.00	0.446	83.33
42.00	0.091	#DIV/0!	80.00	0.458	71.43
43.00	0.091	1000.00	81.00	0.472	71.43
44.00	0.092	#DIV/0!	82.00	0.486	58.82
45.00	0.092	1000.00	83.00	0.503	50.00
46.00	0.093	500.00	84.00	0.523	21.28
47.00	0.095	111.11	85.00	0.570	21.28
48.00	0.104	200.00	86.00	0.617	10.99
49.00	0.109	24.39	87.00	0.708	22.22
50.00	0.150	33.33	88.00	0.753	12.99
51.00	0.180	33.33	89.00	0.830	50.00
52.00	0.210	55.56	90.00	0.850	58.82
53.00	0.228	52.63	91.00	0.867	25.64
54.00	0.247	62.50	92.00	0.906	35.71
55.00	0.263	125.00	93.00	0.934	15.63
56.00	0.271	76.92	94.00	0.998	250.00
57.00	0.284	125.00	95.00	1.002	11.36
58.00	0.292	125.00	96.00	1.090	66.67
59.00	0.300	142.86	97.00	1.105	10.75
60.00	0.307	142.86	98.00	1.198	3.91
			99.00	1.454	68.09

11-16 cm		
% Less Than	size (um)	Differential
85.00	0.092	12.35
86.00	0.173	9.26
87.00	0.281	31.25
88.00	0.313	37.04
89.00	0.34	2.38
90.00	0.76	-3.36
91.00	0.462	16.95
92.00	0.521	19.61
93.00	0.572	23.26
94.00	0.615	21.28
95.00	0.662	20.00
96.00	0.712	18.52
97.00	0.766	15.15
98.00	0.832	11.49
99.00	0.919	107.73

Sonicated Silt-Size Aggregate

Silt Aggregates Sonicated

600 J				2000 J			
	% Less Than	Size (um)	Differential		% Less Than	Size (um)	Differential
11-16 cm	71.00	0.0710	8.47	3-5 cm	97.00	0.0740	1000.00
	72.00	0.1890	58.82		98.00	0.0750	1000.00
	73.00	0.2060	66.67		99.00	0.0760	166.67
	74.00	0.2210	58.82	7-9 cm	93.00	0.0400	500.00
	75.00	0.2380	29.41		94.00	0.0420	500.00
	76.00	0.2720	166.67		95.00	0.0440	500.00
	79.00	0.2900	100.00		96.00	0.0460	1000.00
	81.00	0.3100	400.00		97.00	0.0470	500.00
	85.00	0.3200	66.67		98.00	0.0490	10000.00
	87.00	0.3500	300.00		99.00	0.0491	20000.00
	90.00	0.3600	100.00	9-11 cm	77.00	0.0480	500.00
	94.00	0.4000	50.00		78.00	0.0500	1000.00
	99.00	0.5000	198.00		79.00	0.0510	1000.00
					80.00	0.0520	1000.00
					81.00	0.0530	1000.00
					82.00	0.0540	142.86

1000 J			
	% Less Than	Size (um)	Differential
5-7 cm	88.00	0.0180	500.00
	89.00	0.0200	500.00
	90.00	0.0220	500.00
	91.00	0.0240	500.00
	92.00	0.0260	500.00
	93.00	0.0280	500.00
	94.00	0.0300	52.63
	95.00	0.0490	500.00
	96.00	0.0510	1882.35

9-11 cm	83.00	0.0610	1000.00
	84.00	0.0620	1000.00
	85.00	0.0630	2000.00
	86.00	0.0635	2000.00
	87.00	0.0640	909.09
	88.00	0.0651	5000.00
	89.00	0.0653	1666.67
	90.00	0.0659	10000.00
	91.00	0.0660	1000.00
	92.00	0.0670	10000.00
	93.00	0.0671	1111.11
	94.00	0.0680	10000.00
	95.00	0.0681	1111.11
	96.00	0.0690	1000.00
	97.00	0.0700	2000.00
	98.00	0.0705	2000.00
	99.00	0.0710	1394.37

VITA

Laura Ann Taylor was born in `982 in Greenbrae, California. After spending much of her childhood in Portland, Oregon she moved to Albuquerque, New Mexico. Laura graduated from Valley High School in 2000. She then earned a B.S. in Environmental Science from the University of Denver in 2003. She received her M.S. in Geology from the University of Tennessee, Knoxville in 2007.

Laura is currently employed as an environmental scientist with Tetra Tech, Inc. in Oak Ridge, Tennessee.

5324 7016 8
06/11/08 VA